




Leptin modulates pancreatic β -cell membrane potential through Src kinase–mediated phosphorylation of NMDA receptors

Received for publication, August 3, 2020, and in revised form, October 8, 2020. Published, Papers in Press, October 9, 2020, DOI 10.1074/jbc.RA120.015489

Veronica A. Cochrane¹, Yi Wu¹, Zhongying Yang¹, Assmaa ElSheikh^{1,2}, Jeremy Dunford³, Paul Kievit⁴, Dale A. Fortin^{1,3,*}, and Show-Ling Shyng^{1,*} 

From the ¹Department of Chemical Physiology and Biochemistry, Oregon Health and Science University, Portland, Oregon, USA, the ²Department of Medical Biochemistry, Tanta University, Tanta, Egypt, the ³Department of Integrated Physiology and Neuroscience, College of Arts and Sciences, Washington State University, Vancouver, Washington, USA, and the ⁴Division of Cardiometabolic Health, Oregon National Primate Research Center, Beaverton, Oregon, USA

Edited by Roger J. Colbran

The adipocyte-derived hormone leptin increases trafficking of K_{ATP} and Kv2.1 channels to the pancreatic β -cell surface, resulting in membrane hyperpolarization and suppression of insulin secretion. We have previously shown that this effect of leptin is mediated by the NMDA subtype of glutamate receptors (NMDARs). It does so by potentiating NMDAR activity, thus enhancing Ca^{2+} influx and the ensuing downstream signaling events that drive channel trafficking to the cell surface. However, the molecular mechanism by which leptin potentiates NMDARs in β -cells remains unknown. Here, we report that leptin augments NMDAR function via Src kinase–mediated phosphorylation of the GluN2A subunit. Leptin-induced membrane hyperpolarization diminished upon pharmacological inhibition of GluN2A but not GluN2B, indicating involvement of GluN2A-containing NMDARs. GluN2A harbors tyrosine residues that, when phosphorylated by Src family kinases, potentiate NMDAR activity. We found that leptin increases phosphorylation of Tyr-418 in Src, an indicator of kinase activation. Pharmacological inhibition of Src or overexpression of a kinase-dead Src mutant prevented the effect of leptin, whereas a Src kinase activator peptide mimicked it. Using mutant GluN2A overexpression, we show that Tyr-1292 and Tyr-1387 but not Tyr-1325 are responsible for the effect of leptin. Importantly, β -cells from *db/db* mice, a type 2 diabetes mouse model lacking functional leptin receptors, or from obese diabetic human donors failed to respond to leptin but hyperpolarized in response to NMDA. Our study reveals a signaling pathway wherein leptin modulates NMDARs via Src to regulate β -cell excitability and suggests NMDARs as a potential target to overcome leptin resistance.

Leptin is an adipocyte-produced hormone that plays a key role in body weight regulation. The physiological actions and signaling mechanisms of leptin in the central nervous system have been extensively studied. Less well-understood is the function and mechanism of leptin signaling in peripheral tissues. In pancreatic islets, leptin was reported to down-regulate glucose-stimulated insulin secretion more than 2 decades

ago (1–6). Recent studies find that leptin stimulates potassium channel trafficking to the cell surface to reduce β -cell excitability (7–9). Specifically, leptin causes a transient increase in the number of ATP-sensitive potassium (K_{ATP}) channels and Kv2.1 channels in the β -cell plasma membrane (9). K_{ATP} channels control β -cell resting membrane potential and couple blood glucose with insulin secretion, whereas Kv2.1 channels play a prominent role in action potential repolarization to stop insulin secretion (10, 11). The increased surface abundance of these channels would reduce β -cell excitability and thus explain how leptin inhibits glucose-stimulated insulin secretion.

Leptin signaling is complex, and multiple signal transduction pathways have been described (12, 13). The best-characterized is JAK2-dependent phosphorylation of STAT3 following activation of the ObRb receptor, but phosphatidylinositol 3-kinase/Akt, mitogen-activated protein kinase, AMPK, and Src family kinases (SFKs) are also possible downstream effectors (13, 14). In addition, transactivation of other cytokine receptors via leptin signaling has also been implicated (13). Studies into the mechanisms by which leptin regulates K_{ATP} and Kv2.1 channel trafficking so far have identified several key molecular players. These include the NMDA subtype glutamate receptors (NMDARs), calcium/calmodulin-dependent protein kinase kinase β (CaMKK β), AMPK, and PKA (15). Evidence that has emerged reveals a novel signaling pathway wherein leptin potentiates NMDAR function to increase Ca^{2+} influx, resulting in activation of CaMKK β , which phosphorylates and activates AMPK; AMPK in turn causes PKA-dependent actin depolymerization, culminating in increased trafficking of K_{ATP} and Kv2.1 channels to the β -cell surface. A key question of how leptin potentiates NMDAR activity, however, has yet to be addressed.

NMDARs are calcium-permeant ionotropic glutamate receptors that are highly expressed in the brain and are important for learning and memory (16). Although they are extensively studied in the central nervous system, there is growing evidence that they are expressed in pancreatic β -cells and play a role in regulating insulin secretion (17–19). Functional NMDARs generally form as heterotetramers of two obligatory glycine-binding GluN1 subunits (also known as NR1) and two

* For correspondence: Show-Ling Shyng, shyngs@ohsu.edu; Dale A. Fortin, dale.fortin@wsu.edu.

Leptin and GluN2A phosphorylation in β -cells

glutamate-binding GluN2 (GluN2A-D or NR2A-D) subunits (20). NMDARs containing GluN2A and -2B subunits are highly sensitive to blockade by extracellular Mg^{2+} under negative membrane potential and require membrane depolarization to remove Mg^{2+} block for activity, whereas those with GluN2C and -2D subunits are significantly less sensitive to external Mg^{2+} (16, 20, 21). Additionally, NMDAR activity can be modulated by post-translational modifications. In particular, GluN2A and GluN2B have long cytoplasmic tails that are known to be phosphorylated at serine/threonine and/or tyrosine residues by a variety of kinases, including CDK5, PKA, PKC, CaMKII, casein kinase II, and protein tyrosine kinases (22). In neurons, these phosphorylation modifications have been linked to regulation of NMDAR trafficking, localization, and function (reviewed in Ref. 23). For example, phosphorylation of several tyrosine residues in GluN2A by SFKs have been shown to enhance NMDAR activity (24, 25). Of note, Src activation is one of the many downstream signaling events that have been reported following stimulation of the OBRb leptin receptor by leptin (14, 26, 27), raising the possibility that leptin may signal through SFKs to modulate NMDAR activity in pancreatic β -cells.

Here, we present evidence that leptin activates Src to phosphorylate GluN2A-containing NMDARs in pancreatic β -cells, which results in potentiation of NMDAR currents and increased trafficking of K_{ATP} and Kv2.1 channels to the cell surface to hyperpolarize β -cell membrane potential. Importantly, we show that leptin fails to induce membrane hyperpolarization in β -cells from the leptin-resistant *db/db* mice and obese diabetic human donors. Interestingly, direct activation of NMDARs by NMDA was able to mimic the effect of leptin. As leptin resistance is frequently associated with obesity-related diabetes, NMDARs may be a potential target to overcome leptin resistance in diabetic β -cells.

Results

Leptin hyperpolarizes pancreatic β -cells through GluN2A-containing NMDARs

In rodent pancreatic β -cell lines as well as primary human β -cells, leptin induces membrane hyperpolarization at glucose concentrations that depolarize β -cell membrane potential (3, 7–9, 19). Recently, we showed that, both in rat insulinoma INS-1 832/13 cells and human β -cells, this effect is mediated by NMDARs (19). Leptin stimulation increased NMDA currents, leading to increased Ca^{2+} influx and increased surface density of K_{ATP} and Kv2.1 channels (19). To determine the mechanism by which leptin increases NMDA currents, we began by characterizing the NMDARs that are expressed in β -cells. Functional NMDARs that are Ca^{2+} -permeant are tetramers of two GluN1 subunits and two of four different GluN2 subunits, GluN2A, -2B, -2C, and -2D (20). The GluN1 subunit is obligatory and is encoded by a single gene, *Grin1*. In contrast, GluN2 subunits are encoded by four different genes: *Grin2a*, *Grin2b*, *Grin2c*, and *Grin2d* for GluN2A–D (20). We first examined the expression of these subunits at the mRNA level in INS-1 832/13 cells by RT-PCR. Transcripts for *Grin1*, *Grin2a*, *Grin2b*, and *Grin2d* were clearly detected, but not *Grin2c* (Fig. 1A), suggesting that

these cells express GluN1, GluN2A, GluN2B, and GluN2D, but not GluN2C.

NMDARs containing GluN2A or -2B are much more sensitive to external Mg^{2+} block than those containing GluN2C or -2D (20, 28). We thus tested Mg^{2+} sensitivity of NMDA currents using whole-cell recording as an indicator of the GluN2 subunit composition. Puff application of NMDA (1 mM) at a holding potential of -70 mV in Mg^{2+} -free external solution elicited NMDA currents that were reduced by $>80\%$ upon the addition of $MgCl_2$ (100 μM) to the external solution (from 11.3 ± 2.6 to 1.3 ± 0.5 pA, $n = 4$; $p < 0.05$ by paired *t* test) (Fig. 1, B and C). The strong Mg^{2+} block observed is characteristic of NMDARs containing GluN2A and/or GluN2B subunits (21, 28), suggesting that NMDARs at the surface of these cells are largely made up of GluN1 and GluN2A and/or GluN2B subunits. Consistently, in Western blotting experiments, GluN1 and GluN2A were readily detectable in total cell lysate and further enriched in the membrane fraction, whereas GluN2B was barely detectable in total cell lysate but clearly seen in the membrane fraction (Fig. 1D).

Because both GluN2A and -2B could potentially mediate the leptin response, we sought to determine their relative contributions using subunit-specific inhibitors: TCN-201 for GluN2A and Ro 25-6981 for GluN2B (20, 29, 30). Hyperpolarization of membrane potential in Tyrode's solution containing 11 mM glucose was used as a readout for leptin response. Because GluN2A inhibition by TCN-201 depends on glycine, which at higher concentrations renders the drug less effective (30), we reduced the glycine supplement in Tyrode's solution from 100 to 50 μM . These experiments were performed using cell-attached current-clamp recording, which provides a robust assessment of changes in membrane potential while maintaining cell integrity and preventing dialysis of soluble factors that may be important for intracellular signaling (31, 32). Bath application of leptin alone (10 nM) induced a mean membrane hyperpolarization of -46.8 ± 8.1 mV, similar to that reported previously (9, 19). However, co-application of the GluN2A-selective antagonist TCN-201 (50 μM) with leptin only induced a mean hyperpolarization of -14.4 ± 3.9 mV, significantly less than that observed in cells treated with leptin alone (Fig. 1, E and F). By contrast, co-application of the GluN2B-selective antagonist Ro 25-6981 (33) had little effect on the ability of leptin to hyperpolarize INS-1 832/13 cells (Ro 25-6981 at 1 μM , $\Delta V_m = -35.8 \pm 3.8$ mV; Fig. 1, E and F). These results suggest that GluN2A is largely responsible for mediating the effect of leptin. Note that there is evidence that GluN2A can form diheteromeric GluN1/GluN2A or triheteromeric GluN1/GluN2A/GluN2B complexes (20). Because the potency and efficacy of TCN-201 and Ro 25-6981 have been shown to be reduced for triheteromeric GluN1/GluN2A/GluN2B channels, especially for Ro 25-6981 (29, 34), the lack of effect by Ro 25-6981 in our experiment does not allow us to exclude the involvement of GluN1/GluN2A/GluN2B heteromers, as both GluN2A and GluN2B (albeit less abundant compared with GluN2A based on Western blotting of total cell lysate) were detected in membrane fractions prepared from INS-1 832/13 cells by Western blotting (Fig. 1D).

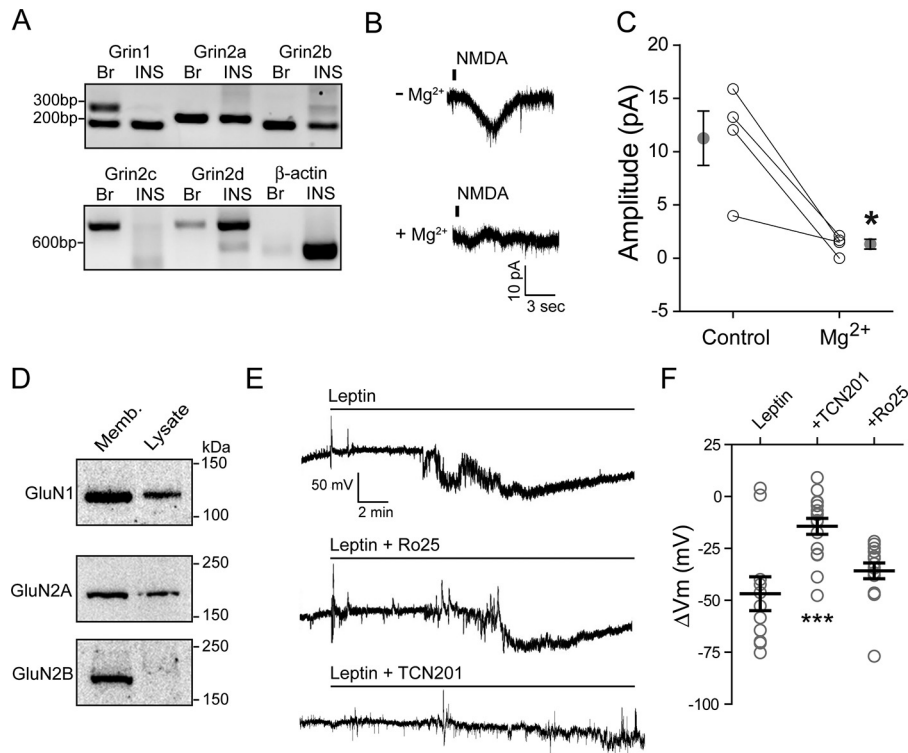


Figure 1. Leptin induces membrane hyperpolarization through GluN2A-containing NMDARs. *A*, RT-PCR detection of mRNA for NMDAR subunits, GluN1 (*Grin1*), GluN2A (*Grin2a*), GluN2B (*Grin2b*), GluN2C (*Grin2c*), and GluN2D (*Grin2d*), in rat brain (*Br*) and INS-1 832/13 cells (*INS*). β -Actin was included as a control. *B*, representative traces of NMDAR currents in the absence (*top*) or presence (*bottom*) of 100 μ M Mg^{2+} . *C*, sensitivity of NMDA currents (elicited by puff application of 1 mM NMDA) to Mg^{2+} block. Averaged current amplitudes before (control) and after 100 μ M Mg^{2+} for each cell are connected by a straight line. Mean \pm S.E. values for each group are shown next to individual data points. *, $p < 0.05$ by paired *t* test. *D*, Western blots showing protein expression of GluN1, GluN2A, and GluN2B from INS-1 832/13 cell membrane fraction (*Memb*; 30 μ g) and total cell lysate (*Lysate*; 30 μ g). *E*, individual cell-attached membrane recordings from INS-1 832/13 cells treated with leptin (10 nM) alone (*top*), with leptin plus the GluN2B inhibitor Ro 25-6981 (middle; Ro25, 1 μ M), or with leptin plus the GluN2A inhibitor TCN201 (*bottom*; 50 μ M). *F*, group data showing the degree of membrane hyperpolarization in mV for leptin alone ($n = 11$ cells) or leptin co-applied with Ro 25-6981 ($n = 14$ cells) or TCN201 ($n = 16$ cells). Here and in subsequent figures, individual cells are represented by symbols and means are indicated by a black line. Error bars, S.E. ***, $p < 0.0005$ by unpaired *t* test as compared with leptin.

Leptin regulates NMDAR activity via Src family kinases

In contrast to GluN1, which has a relatively small cytoplasmic domain of ~ 100 amino acids, GluN2A has a long cytoplasmic tail of ~ 600 amino acids that contains potential phosphorylation sites for a number of protein kinases, including PKA, PKC, CDK5, and the SFKs (22). Phosphorylation by PKC (35), CDK5 (36), and Src (25, 37) in particular has been reported to potentiate NMDAR currents. We therefore monitored changes in INS-1 832/13 cell membrane potentials in response to leptin in the absence or presence of inhibitors for the various kinases. Neither roscovitine (*Ros*; 10 μ M), an inhibitor of CDK5 kinase, nor Go 6983 (*Go*; 10 μ M), a broad-spectrum PKC kinase inhibitor, had significant effects on leptin-induced hyperpolarization ($\Delta V_m = -32.4 \pm 4.1$ mV for leptin alone; $\Delta V_m = -39.3 \pm 7.0$ mV for roscovitine plus leptin; $\Delta V_m = -33.7 \pm 5.5$ mV for Go 6983 plus leptin; Fig. 2, *A* and *B*). By contrast, AZD0530 (AZD; 10 μ M), also known as saracatinib (38), a broad-spectrum inhibitor of SFKs, markedly reduced the ability of leptin to induce membrane hyperpolarization ($\Delta V_m = -4.8 \pm 3.1$ mV, $p < 0.0005$ compared with leptin alone; Fig. 2, *A* and *B*) but had no effect on membrane hyperpolarization triggered by direct activation of NMDARs via NMDA (NMDA: $\Delta V_m = -35.3 \pm 8.9$ mV, $n = 7$; NMDA plus AZD0530: $\Delta V_m = -30.4 \pm 9.9$ mV, $n = 7$). Another tyrosine kinase inhibitor, dasatinib (*Das*; 25 μ M)

(38) also abrogated the effect of leptin, resulting in only a small hyperpolarization ($\Delta V_m = -7.0 \pm 2.4$ mV, $p < 0.0005$ compared with leptin alone; Fig. 2*B*). These results indicate that SFKs but not CDK5 nor PKC are likely involved in the leptin-induced membrane hyperpolarization observed in INS-1 832/13 cells.

Next, we determined whether activation of SFKs via an activating phosphopeptide EPQpYEEIPIYL (referred to as YEEI), which binds to the Src homology 2 domain to relieve kinase autoinhibition (39, 40), could mimic the effects of leptin and induce membrane hyperpolarization. For these experiments, whole-cell current-clamp recordings of INS-1 832/13 cells were carried out to apply YEEI intracellularly through the patch pipette. Under whole-cell conditions with 5 mM ATP in the pipette solution (estimated intracellular [ATP] with 11 mM glucose in the bath solution), inclusion of YEEI phosphopeptide induced significant membrane hyperpolarization ($\Delta V_m = -21.1 \pm 4.1$ mV from break-in to steady state, $n = 7$) compared with the control without the peptide ($\Delta V_m = -4.9 \pm 4.0$ mV from break-in to steady state, $n = 6$) (Fig. 2, *C* and *D*). The result supports the notion that direct activation of SFKs is sufficient to mimic the effect of leptin and cause β -cell membrane hyperpolarization.

To directly test whether SFKs underlie the potentiation of NMDAR currents by leptin, we performed whole-cell recording

Leptin and GluN2A phosphorylation in β -cells

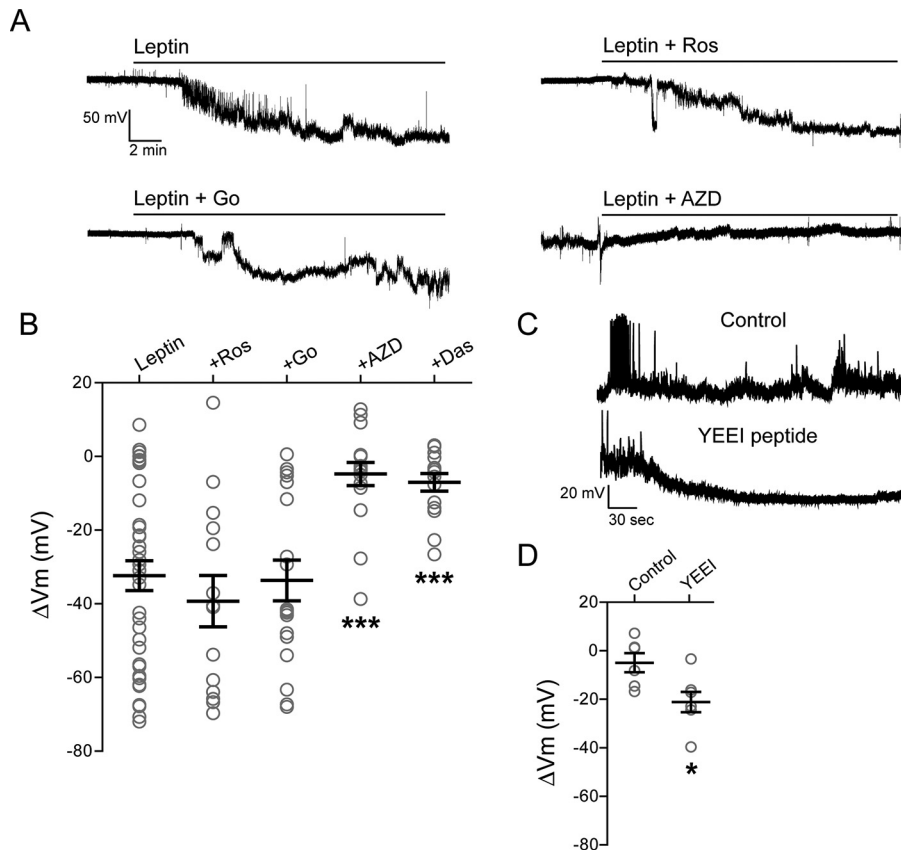


Figure 2. Leptin regulates NMDAR activity via Src family kinases. *A*, representative cell-attached current-clamp recordings from INS-1 832/13 cells treated with leptin (10 nM) alone (*top left*) or leptin with the PKC inhibitor Go 6983 (*bottom left*; Go, 10 μ M), the CDK5 inhibitor roscovitine (*top right*; Ros, 10 μ M), or the SFK inhibitor AZD (*bottom right*; 10 μ M). Inhibitors were applied for 10 min prior to the application of leptin and remained in the solution throughout the recording. *B*, group data showing extent of membrane hyperpolarization for leptin alone ($n = 40$ cells), and leptin co-applied with roscovitine (Ros, $n = 14$), Go 6983 ($n = 18$), AZD ($n = 17$), or dasatinib (Das, 25 μ M; $n = 15$). ***, $p < 0.0005$ by unpaired t test as compared with leptin. *C*, representative whole-cell current-clamp recordings of INS-1 832/13 cells without (*top trace*) or with (*bottom trace*) the Src kinase-activating peptide YEEI (1 μ M) in the pipette solution. *D*, group data showing the degree of hyperpolarization for control ($n = 6$) and YEEI peptide ($n = 7$). *, $p < 0.05$, unpaired t test as compared with control.

of NMDAR currents and monitored how current amplitudes were affected by leptin and the SFK inhibitor AZD0530. In the absence of leptin, repeated puff applications of 1 mM NMDA at 1-min intervals elicited NMDAR currents of similar amplitudes. Bath application of 10 nM leptin potentiated NMDA-evoked currents within 5 min of leptin treatment from a baseline of 14.8 ± 8.0 pA to 25.8 ± 13.3 pA ($p < 0.05$ by Friedman's test; Fig. 3), as we reported previously (19). Subsequent co-application of 10 μ M AZD0530 with leptin abolished the effect of leptin, with averaged NMDA currents of 15.5 ± 8.7 pA comparable with baseline values (Fig. 3). These results provide direct evidence that leptin-mediated potentiation of NMDAR currents requires SFKs.

Leptin modulation of NMDAR activity requires phosphorylation of GluN2A at Tyr-1292 and Tyr-1387

SFKs have been reported to potentiate NMDAR currents by phosphorylating GluN2 (23, 41, 42). Specifically, three tyrosine residues in GluN2A (Tyr-1292, Tyr-1325, and Tyr-1387) have been identified as targets of SFK-mediated phosphorylation to enhance NMDAR function in different experimental systems (24, 25, 41, 43). To determine whether these sites play a role in leptin-induced membrane hyperpolarization, we mutated the three tyrosine residues in GluN2A to phenylala-

nines together GluN2A^{Y1292F,Y1325F,Y1387F} as well as individually (GluN2A^{Y1292F}, GluN2A^{Y1325F}, and GluN2A^{Y1387F}). To facilitate visualization of expression, a GluN2A construct fused to GFP at its extracellular N terminus was used (44). INS-1 832/13 cells were then transfected to express WT or phosphomutants. To confirm that exogenously expressed GFP-GluN2A co-assembles with endogenous GluN1, we performed co-immunoprecipitation experiments using an anti-GFP nanobody. Both GluN1 and GFP-GluN2A were present in the immunoprecipitate as detected by anti-GFP, anti-GluN2A, and anti-GluN1 antibodies in Western blots (Fig. 4A), indicating association of transfected GluN2A with endogenous GluN1. Surface staining of the GFP tag further demonstrates that transfected WT and mutant GluN2A were expressed in the plasma membrane (Fig. 4B).

Changes in membrane potential following leptin treatment were again monitored using cell-attached current-clamp recording. We first compared cells expressing GFP-GluN2A^{WT} with those expressing the GFP-GluN2A^{Y1292F,Y1325F,Y1387F} triple phenylalanine mutant. GFP-negative cells on the same coverslip were also examined as untransfected controls. Representative membrane potential traces from untransfected cells and cells expressing GFP-GluN2A^{WT} or triple phosphomutant GFP-GluN2A^{Y1292F,Y1325F,Y1387F} are shown in Fig. 4C. Leptin

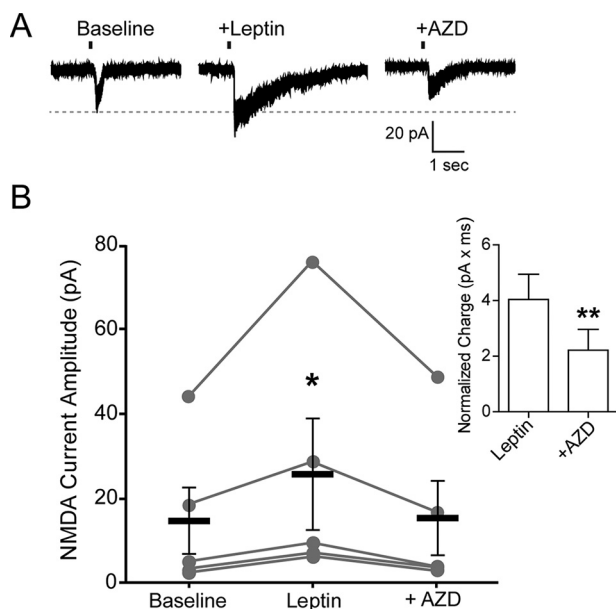


Figure 3. Leptin potentiation of NMDAR currents is prevented by inhibition of Src kinases. *A*, example of whole-cell currents from a single INS-1 832/13 cell induced by puff application of NMDA (1 mM; vertical line indicates time of puff) during baseline, 5 min after leptin, and following wash-in of AZD (10 μ M AZD0350) in the presence of leptin for 5 min. *B*, within-cell group data showing amplitude of NMDAR currents for each condition ($n = 5$ cells). Means for each condition are depicted as thick black lines \pm S.E. (error bars). Statistical analysis was conducted using Friedman's test ($p = 0.0239$) followed by a post hoc Dunn's multiple-comparison test with significance set to $p < 0.05$ (*), as compared with baseline. *Inset*, comparison of total charge (pA \times ms) observed for each NMDA puff between leptin and leptin + AZD treatments normalized to baseline. **, $p < 0.005$, paired Student's t test as compared with leptin.

application to untransfected cells induced a mean hyperpolarization of -51.1 ± 5.6 mV ($n = 10$) that was not statistically significantly different from leptin responses in cells expressing GluN2A^{WT} (-48.0 ± 6.5 mV, $n = 13$). By contrast, leptin had little hyperpolarizing effect in cells expressing the triple phosphomutant (Fig. 4, *C* and *D*; GluN2A^{Y1292F,Y1325F,Y1387F} $\Delta V_m = -12.0 \pm 1.7$ mV; $n = 18$; $p < 0.0005$ by unpaired t test compared with untransfected cells). The diminished response is not due to disruption of K_{ATP} channel gating or expression as the K_{ATP} activator diazoxide (200 μ M) was fully able to hyperpolarize cells expressing GluN2A^{Y1292F,Y1325F,Y1387F} ($\Delta V_m = -52.7 \pm 4.9$ mV; $n = 14$) (Fig. 4*D*). Moreover, we tested the response of cells expressing GluN2A^{Y1292F,Y1325F,Y1387F} to NMDA, which we have shown hyperpolarizes cells in the absence of leptin (19). We found that NMDA hyperpolarized INS-1 832/13 cells by an average of -38.8 ± 7.0 mV ($n = 11$), suggesting that the GluN2A phosphomutant also did not disrupt NMDAR expression or function (Fig. 4*D*). To determine the relative contributions of the three tyrosine residues, we next tested the membrane potential response to leptin in cells expressing GluN2A^{Y1292F}, GluN2A^{Y1325F}, or GluN2A^{Y1387F}. In this cohort of cells, leptin application caused a mean hyperpolarization of -47 ± 3.8 mV in untransfected cells ($n = 26$) (Fig. 4, *E* and *F*). Interestingly, leptin still hyperpolarized cells transfected with GluN2A^{Y1325F} ($\Delta V_m = -41.7 \pm 4.1$ mV; $n = 16$), not significantly different from untransfected cells. By contrast, in cells expressing GluN2A^{Y1292F} or GluN2A^{Y1387F}, the response to

leptin was significantly reduced (Fig. 4, *E* and *F*; ΔV_m for GluN2A^{Y1292F} = -17.4 ± 4.1 mV, $n = 19$, and ΔV_m for GluN2A^{Y1387F} = -24.3 ± 4.7 mV, $n = 15$; $p < 0.0005$ by unpaired t test). Taken together, these results identify the tyrosine phosphorylation sites Tyr-1292 and Tyr-1387 in GluN2A as responsible for mediating the leptin effect.

Leptin activates Src kinase in β -cells

The above results suggest that leptin likely activates SFKs to modulate NMDAR currents. Studies of GluN2A phosphorylation using *in vitro* or the HEK293 cell heterologous expression systems have found that both Src and Fyn can phosphorylate GluN2A (24). Src, when activated, autophosphorylates a highly conserved tyrosine residue, Tyr-418, in the catalytic domain of Src kinase, which is required for its full catalytic activity (45, 46). Increased phosphorylation of Tyr-418 is therefore indicative of kinase activation. We used an antibody raised against a peptide containing Src-pY418 to monitor Src phosphorylation to directly test whether leptin activates Src. Immunocytochemistry experiments were carried out on INS-1 832/13 cells treated with or without leptin (10 nM for 10 min) in the presence or absence of the tyrosine kinase inhibitor dasatinib (50 μ M). We found that leptin induced a significant increase in Src-pY418 staining as compared with matched controls with prominent staining at the cell periphery (Fig. 5, *A* and *B*) that was inhibited by co-application of dasatinib (Fig. 5, *A* and *B*). Further biochemical experiments using similar treatment conditions were carried out. In good agreement with the immunostaining results, leptin increased the ratio of phosphorylated to total Src by $176.0 \pm 30.0\%$ as compared with controls ($p < 0.05$ by unpaired t test), which was reduced to $102.1 \pm 40.4\%$ of controls when co-applied with dasatinib (Fig. 5, *C* and *D*). Because the Src-pY418 antibody also recognizes conserved corresponding phosphopeptide in other SFKs, including Fyn, and because both Src and Fyn are expressed in β -cells (47), we further tested the requirement of Src activity in leptin-induced response by expressing a dominant-negative kinase-dead Src mutant (48) (see "Experimental procedures") in INS-1 832/13 cells. For this, we monitored leptin-induced increase of K_{ATP} channel surface expression by surface biotinylation, as described in our previous studies (7, 9). As expected, leptin caused an increase in surface biotinylated SUR1, the regulatory subunit of the β -cell K_{ATP} channel, in control cells. However, in cells transfected with the kinase-dead Src mutant leptin failed to show an increase in surface biotinylated SUR1 (Fig. 5, *E* and *F*). This result lends further support to the requisite role of Src activity in mediating the effect of leptin on K_{ATP} channel trafficking.

Leptin signaling through Src-mediated phosphorylation of GluN2A is conserved in human β -cells

We have previously shown that leptin induces hyperpolarization that depends on NMDARs in human β -cells as in INS-1 832/13 cells (19). Having found that leptin potentiates NMDARs via Src-mediated phosphorylation of GluN2A in INS-1 832/13 cells, we next tested whether the same mechanism applies to human β -cells. Cell-attached current-clamp recordings were made in human β -cells dissociated from islets

Leptin and GluN2A phosphorylation in β -cells

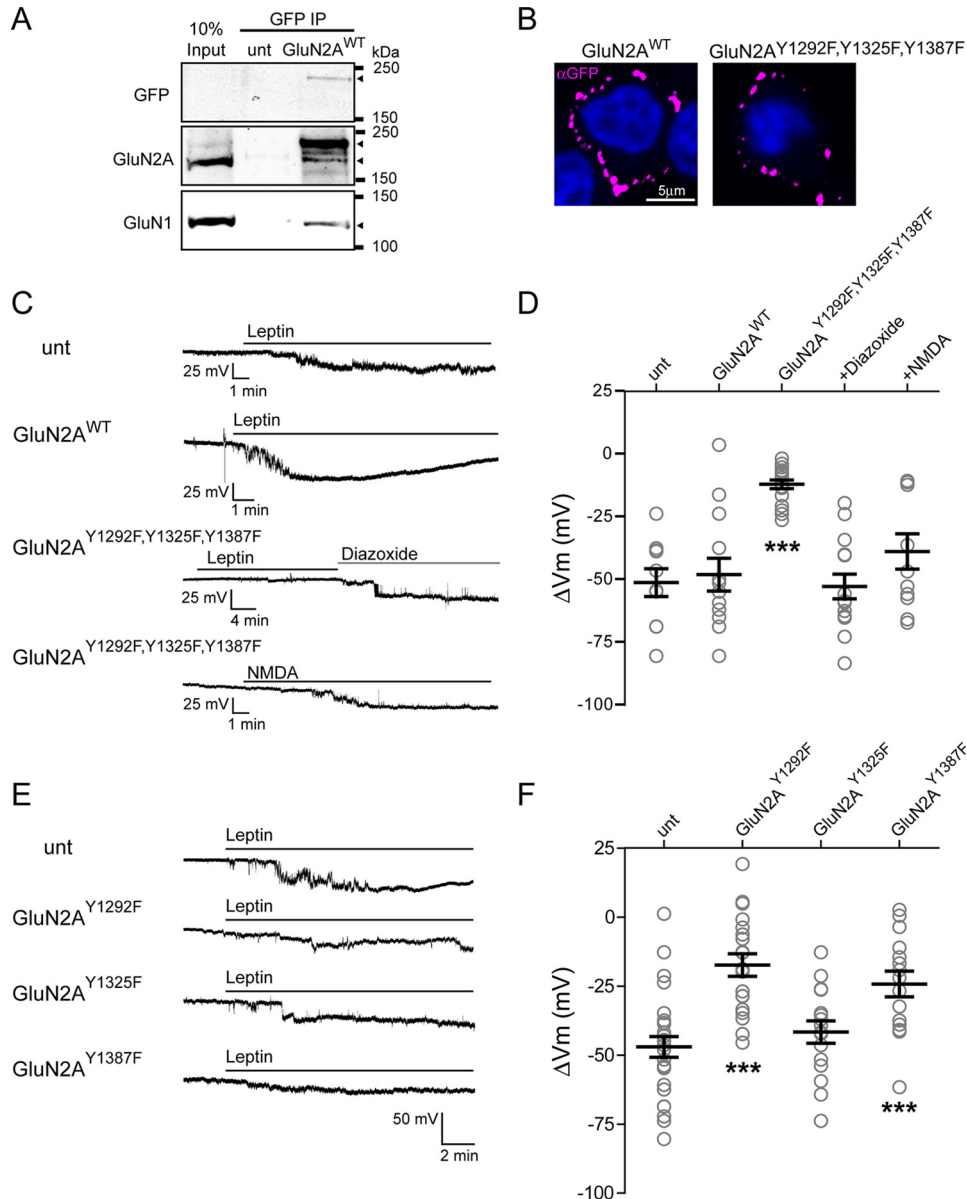


Figure 4. Leptin-induced membrane hyperpolarization requires phosphorylation of GluN2A Tyr-1292 and Tyr-1387 but not Tyr-1325. *A*, immunoprecipitation of GFP-GluN2A with anti-GFP followed by immunoblotting using anti-GFP, anti-GluN2A, or anti-GluN1 antibodies showing association of endogenous GluN2A and GluN1 with transfected GFP-GluN2A. Arrowheads next to the blots indicate protein bands corresponding to GFP-GluN2A^{WT} (top blot), GFP-GluN2A^{WT} (top arrowhead) and endogenous GluN2A (bottom arrowhead, middle blot), and GluN1 (bottom blot). *B*, surface staining using anti-GFP antibody showing plasma membrane expression of GFP-GluN2A^{WT} and GFP-GluN2A^{Y1292F,Y1325F,Y1387F}. *C*, representative INS-1 832/13 cell-attached current-clamp recordings from an untransfected cell (unt) or a cell transfected with GluN2A^{WT} treated with leptin (10 nM) or cells transfected with GluN2A^{Y1292F,Y1325F,Y1387F} and treated with leptin followed by the K_{ATP} channel activator diazoxide (200 μ M) or with NMDA (50 μ M). All GluN2A constructs in this and subsequent panels contain an N-terminal GFP tag. *D*, group data showing the degree of hyperpolarization induced by leptin in untransfected cells ($n = 10$), cells transfected with GluN2A^{WT} ($n = 13$), and cells transfected with GluN2A^{Y1292F,Y1325F,Y1387F} ($n = 18$) with subsequent exposure to diazoxide (200 μ M; $n = 14$) or treated with NMDA alone (50 μ M; $n = 11$). *E*, representative cell-attached recordings from an untransfected cell and three different GluN2A phosphorylation mutants (Y1292F, Y1325F, or Y1387F) treated with 10 nM leptin. *F*, group data showing the amount of hyperpolarization induced by leptin for an untransfected cell ($n = 26$) and for single GluN2A phosphorylation mutants (GluN2A^{Y1292F}, $n = 19$; GluN2A^{Y1325F}, $n = 16$; GluN2A^{Y1387F}, $n = 15$). ***, $p < 0.0005$ by unpaired t test as compared with untransfected cells. Error bars, S.E.

of three different nondiabetic donors obtained through the Integrated Islets Distribution Program (IIDP). All donor information can be found in Table 1. Bath application of leptin alone induced a mean membrane hyperpolarization of -43.7 ± 8.9 mV ($n = 9$ cells from three donors) (Fig. 6, *A* and *B*). The GluN2A-selective inhibitor TCN-201 largely eliminated the leptin response ($\Delta V_m = -9.1 \pm 4.2$ mV, $n = 12$ cells from 3 donors; $p < 0.05$, unpaired t test) (Fig. 6, *A* and *B*), suggesting

that GluN2A-containing NMDARs underlie leptin signaling in human β -cells. We next tested whether leptin modulation of NMDARs and membrane potential in human β -cells requires Src. As shown in the example traces in Fig. 6C, the SFK inhibitor AZD0530 nearly abolished the ability of leptin to hyperpolarize human β -cells ($\Delta V_m = -0.4 \pm 1.2$ mV; $n = 6$ cells from two nondiabetic donors), whereas another SFK inhibitor, dasatinib, also diminished leptin-induced hyperpolarization, albeit

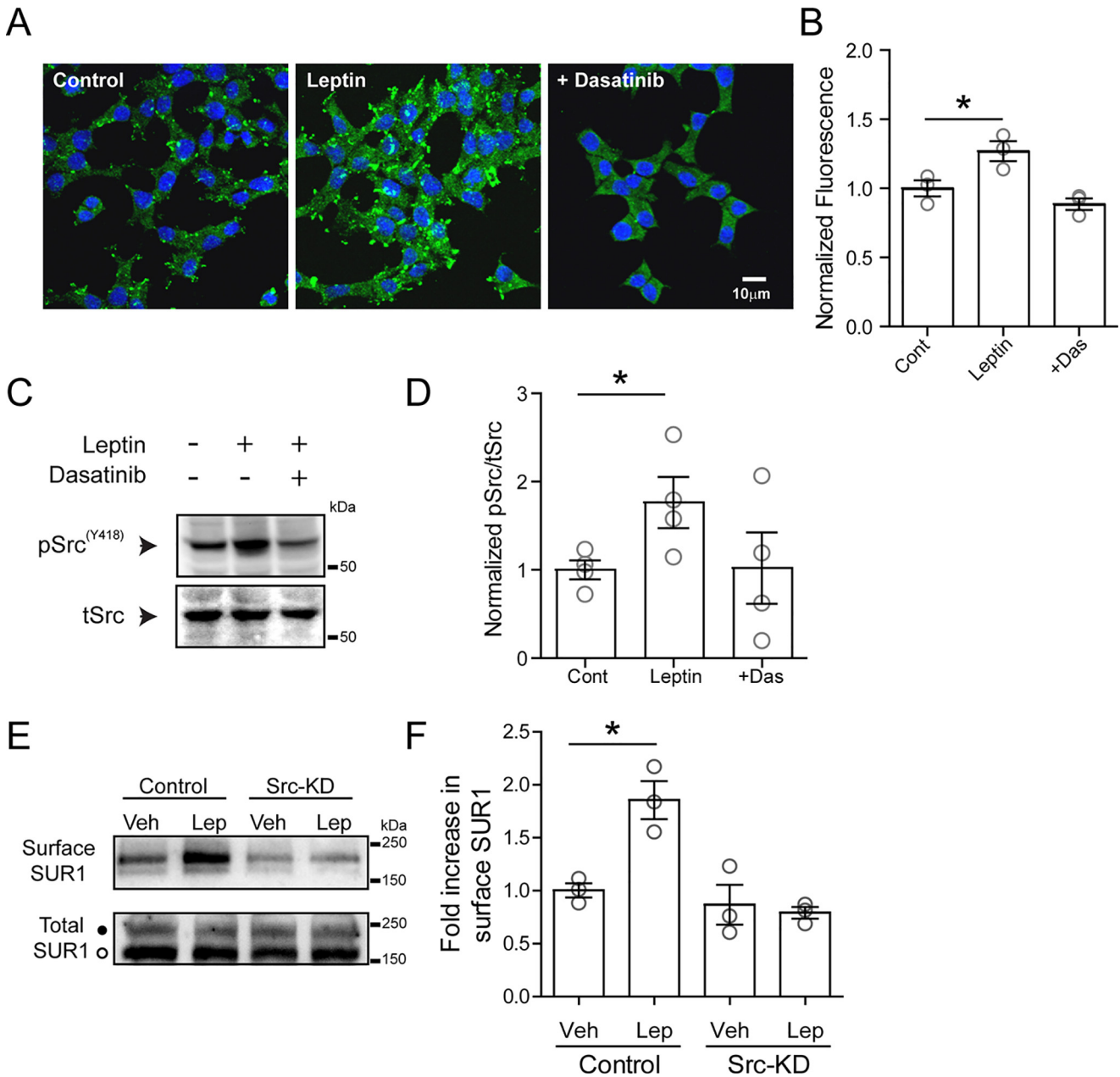


Figure 5. Leptin induces activation of Src kinase. *A*, immunofluorescence images of cultured INS-1 831/13 cells stained with 4',6-diamidino-2-phenylindole (blue) and phosphorylated Src^{Y418} (green) for conditions indicated. Cells were treated with vehicle (control), leptin (10 nM, 10 min), or leptin with dasatinib (25 μ M, pretreated for 30 min before leptin was applied). *B*, group data for phosphorylated Src^{Y418} fluorescence for each condition normalized to the control ($n = 100$ cells/condition for each experiment, and the experiment was repeated three times). *, $p < 0.05$, unpaired Student's t test. *C*, representative Western blotting of phosphorylated Src^{Y418} from cell lysates prepared from INS-1 832/13 cells treated with vehicle, leptin, or leptin co-applied with dasatinib. *D*, group data from four independent experiments as indicated in *C*. *, $p < 0.05$, unpaired Student's t test. *E*, top, Western blotting showing surface SUR1 in response to vehicle or leptin using control cells and cells transfected with an Src kinase-dead mutant (*Src-KD*). Bottom, total SUR1 showing both the complex glycosylated form (top band, solid circle) that can traffic to the cell surface and the core-glycosylated form (bottom band, open circle) that is in the endoplasmic reticulum/early Golgi. *F*, quantitation of three independent surface SUR1 experiments. Data were analyzed by one-way analysis of variance ($p = 0.0019$, $F = 12.95$) followed by a post hoc Dunnett's multiple-comparison test with significance set to $p < 0.05$ (*). Error bars, S.E.

to a lesser extent ($\Delta V_m = -13.5 \pm 2.8$ mV, $n = 7$ cells from three donors) compared with human β -cells treated with leptin alone ($\Delta V_m = -33.5 \pm 6.0$ mV; $n = 17$ cells from five nondiabetic donors; $p < 0.0005$ between AZD0530 and control, and $p < 0.05$ between dasatinib and control, Welch's t test) (Fig. 6D). Taken together, results from both INS-1 832/13 and human β -cells establish a mechanistic link between leptin receptor signaling and modulation of GluN2A-containing NMDARs via Src kinase.

Leptin signaling through NMDARs is disrupted in β -cells from *db/db* mice and from human type 2 diabetic donors

Leptin resistance is a common pathological feature of type 2 diabetes associated with obesity (49). To test how the leptin-signaling pathway pertinent to this study is affected in diabetic β -cells, we examined β -cells from leptin-insensitive *db/db* mice, which harbors a mutation in the leptin receptor gene that renders ObRb signaling-defective (50), as well as from human obese type 2 diabetic donors. Cell-attached recordings of

Leptin and GluN2A phosphorylation in β -cells

Table 1
Human islet donor information

Donor no. (date received) ^a	T2D ^b	Age	Gender	BMI ^c	Cause of death	Islet viability (%)	Islet purity (%)
1 (11/21/17)	N	62	M	28.9	Stroke	97	80
2 (01/10/18)	N	32	M	26.2	Anoxia	98	85
3 (10/09/18)	N	47	F	24.1	Stroke	90	90
4 (10/19/18)	N	55	F	35.7	Stroke	98	94
5 (04/02/18)	N	32	M	32.3	Anoxia	95	85
6 (11/07/18)	N	48	M	24.4	Head trauma	90	90
7 (10/27/15)	Y	41	F	43.1	Stroke	95	95
8 (08/09/16)	Y	52	F	39.9	Anoxia	95	85
9 (08/29/16)	Y	57	M	34.6	Head trauma	98	80
10 (11/07/16)	Y	55	M	32.5	Anoxia	98	75
11 (04/03/17)	Y	65	F	42.6	Anoxia	90	95
12 (06/01/17)	Y	42	F	37.0	Head trauma	89	90
13 (12/13/17)	Y	37	F	38.1	Stroke	94	85

^aDonor information for specific experiments is as follows: Fig. 6B: donors 4, 5, 6; Fig. 6C, D: donors 1, 2, 3, 4, 6; Fig. 8A: donor 7, 8, 9; Fig. 8B, C, D: donors 10, 11; total NMDAR currents from normal β -cells: donors 1, 2, 3, 4, 5; total NMDAR currents from T2D β -cells: donors 12, 13.

^bT2D: type 2 diabetes.

^cBMI: body mass index.

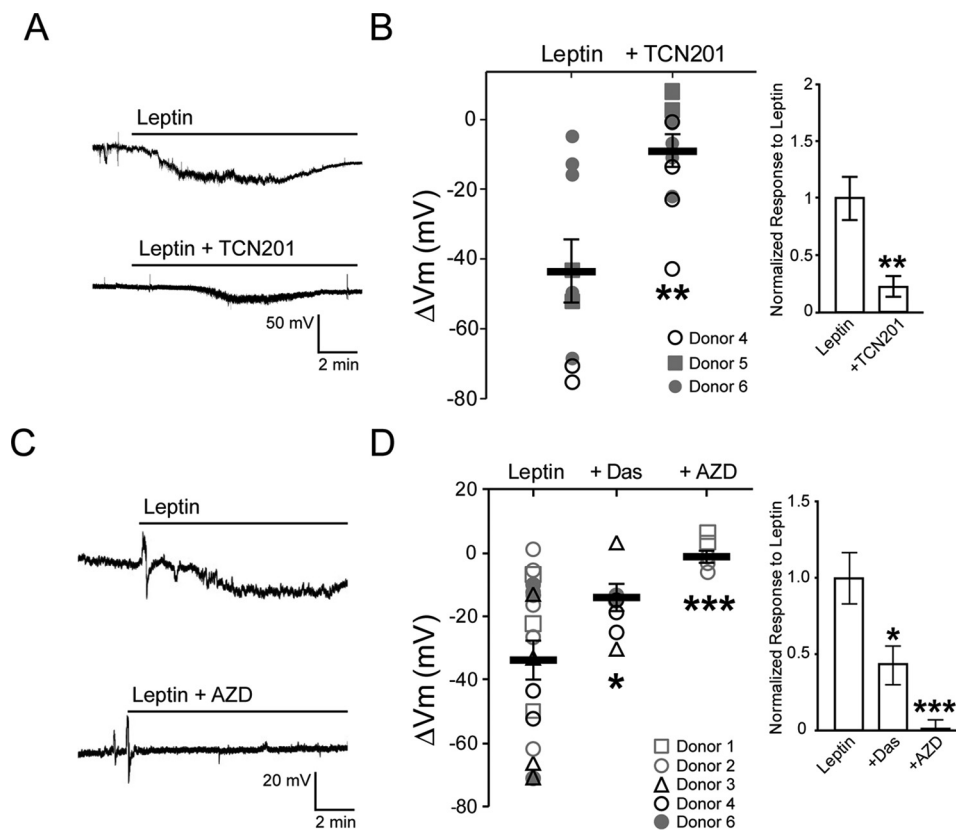


Figure 6. Leptin signaling through GluN2A-containing NMDARs in human β -cells is mediated by Src family kinases. A, individual cell-attached membrane potential recordings from human β -cells isolated from nondiabetic islets treated with leptin (10 nM) alone (top) or leptin together with TCN-201 (bottom; 50 μ M). B, summary data from three nondiabetic donors showing the amount of hyperpolarization induced by leptin alone ($n = 2-5$ cells/donor) or when leptin was co-applied with TCN-201 ($n = 3-4$ cells/donor). Inset, normalized responses to leptin across donors in the absence or presence of TCN-201. C, representative traces of cell-attached current-clamp recordings from human β -cells isolated from nondiabetic islets treated with leptin in the absence or presence of AZD (10 μ M). D, summary data from five nondiabetic donors showing the extent of membrane hyperpolarization in response to leptin alone ($n = 19$ cells; 3-6 cells/donor) or when leptin was co-applied with dasatinib (Das; 25 μ M; $n = 7$ cells; 2-3 cells/donor) or AZD ($n = 6$ cells; 3 cells/donor). Inset, normalized responses to leptin across donors in the absence or presence of dasatinib or AZD. *, $p < 0.05$; ***, $p < 0.0005$, Welch's t test compared with leptin alone group. Error bars, S.E.

membrane potential in β -cells isolated from C57BL/6J (WT) mice showed a clear response to leptin with a ΔV_m of -33.5 ± 5.2 mV ($n = 8$), as expected. By contrast, β -cells isolated from *db/db* mice failed to respond to leptin (10 nM leptin for 15 min, $\Delta V_m = -0.4 \pm 0.4$ mV, $n = 6$, $p < 0.0001$), although subsequent application of the K_{ATP} channel opener diazoxide (250 μ M)

evoked large hyperpolarizations ($\Delta V_m = -44.7 \pm 8.0$ mV, $n = 6$) (Fig. 7, A and B), suggesting that K_{ATP} channels are functionally expressed in these mice. These results also provide clear evidence that leptin-induced hyperpolarization requires functional leptin receptors. Next, we tested whether direct activation of NMDARs using the receptor agonist NMDA can bypass

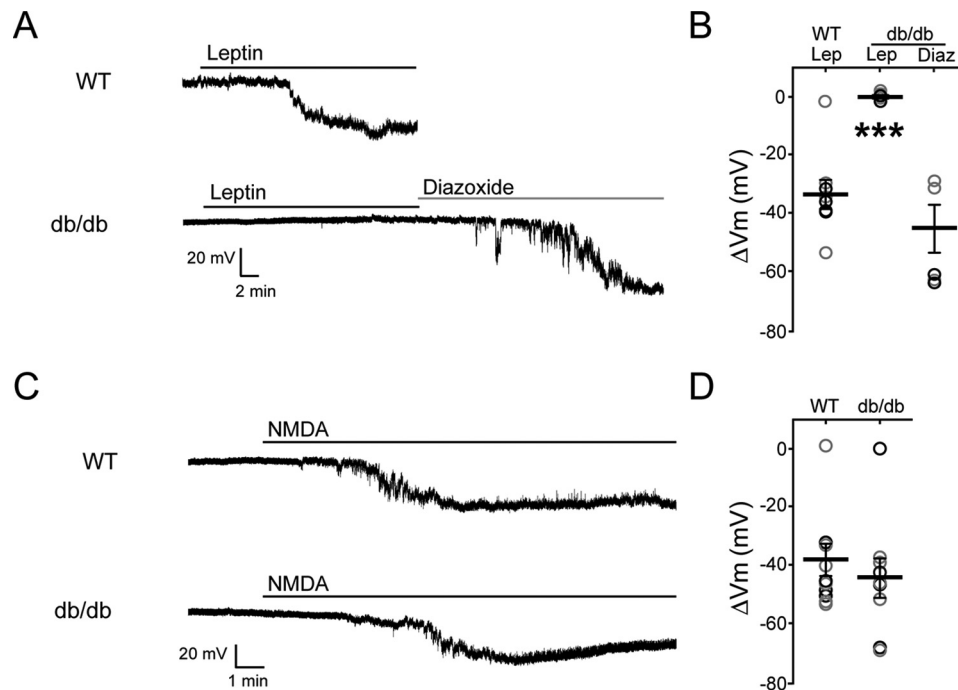


Figure 7. Direct NMDAR activation causes membrane hyperpolarization in mice deficient in leptin receptor signaling. *A*, representative cell-attached membrane potential recordings from β -cells isolated from C57BL/6J (WT) mice treated with leptin (*top trace*) or β -cells isolated from db/db mice treated with leptin (10 nM) followed by diazoxide (250 μ M; *bottom trace*). *B*, group data showing the degree of membrane hyperpolarization in mV for β -cells isolated from C57BL/6J (WT, $n = 9$) or db/db ($n = 7$) mice for the indicated conditions. Gray and black circles indicate different animals. ***, $p < 0.0001$, unpaired Student's *t* test compared with WT leptin-treated group. *C*, as described for *A* except β -cells were treated with NMDA (50 μ M). *D*, group data showing the degree of membrane hyperpolarization in mV for β -cells isolated from C57BL/6J ($n = 9$) or db/db ($n = 9$) mice following NMDA treatment. Error bars, S.E.

leptin receptor deficiency and cause membrane hyperpolarization in the absence of leptin. Control WT cells hyperpolarized in response to bath application of 50 μ M NMDA ($\Delta V_m = -37.9 \pm 5.5$ mV, $n = 9$). Strikingly, β -cells from db/db mice also showed robust responses to NMDA ($\Delta V_m = -44.3 \pm 6.7$ mV, $n = 9$; Fig. 7, *C and D*), indicating that the signaling events downstream of NMDAR activation that lead to increased K_{ATP} and Kv2.1 channel trafficking and membrane hyperpolarization remain intact despite harboring nonfunctional leptin receptors.

To test whether findings from the monogenic leptin-resistant mouse β -cells are also reproduced in human diabetic β -cells, we examined β -cells from obese (body mass index > 30) diabetic donors with presumably different genetic background through the IIDP (see Table 1 for donor information). We first tested whether these cells were resistant to leptin. Whole-cell recordings were performed to assess K_{ATP} and Kv2.1 current density with or without leptin treatment (10 nM for 30 min) as described previously from β -cells taken from normal donors (7, 9). In contrast to normal human β -cells (7, 9), leptin did not increase the current density of K_{ATP} channels (107.4 ± 23.2 for control *versus* 75.4 ± 11.7 pA/pF for leptin-treated, $n = 6$) or Kv2.1 channels (683.3 ± 146.3 for control *versus* 720.3 ± 158.0 pA/pF for leptin-treated, $n = 10$) (Fig. 8*A*). Moreover, leptin failed to potentiate NMDAR currents in β -cells from diabetic donors (12.4 ± 2.3 pA for control *versus* 11.3 ± 1.8 pA following leptin treatment, $n = 5$) (Fig. 8*B*), in contrast to β -cells from normal donors we reported previously (19). Consistent with these results, leptin did not induce mem-

brane hyperpolarization in diabetic human β -cells ($\Delta V_m = 1.3 \pm 2.1$ mV for leptin, $n = 8$) (Fig. 8, *C and D*). Conversely, application of 50 μ M NMDA in the bath solution to directly activate NMDARs in β -cells from the same donors used to test leptin response did induce significant hyperpolarization ($\Delta V_m = -22.0 \pm 8.6$ mV, $n = 9$) (Fig. 8, *C and D*), indicating that NMDAR function and downstream signaling events were not compromised as was observed in β -cells from db/db mice. These results show that β -cells from a sample of obese diabetic donors were leptin-resistant but retained the ability to hyperpolarize in response to direct NMDAR activation.

Discussion

The results presented in this study elucidate the mechanism by which leptin potentiates NMDAR currents to regulate pancreatic β -cell excitability. Multiple lines of evidence support our conclusion that leptin modulation of β -cell membrane potential requires the phosphorylation of GluN2A-containing NMDARs by Src kinase. First, application of TCN-201, a potent and highly selective inhibitor for GluN2A-containing NMDARs, diminished leptin-induced membrane hyperpolarization in both INS-1 832/13 and human β -cells. Second, inhibition of SFKs blocked the ability of leptin to potentiate NMDAR currents and hyperpolarize β -cells. Third, leptin increased phosphorylation of Src at Tyr-418, a site that is required for its catalytic activity (45, 46), and dominant-negative suppression of Src activity via a kinase-dead mutant prevented the ability of leptin to increase surface K_{ATP} channels. Finally, mutation of known Src kinase phosphorylation

Leptin and GluN2A phosphorylation in β -cells

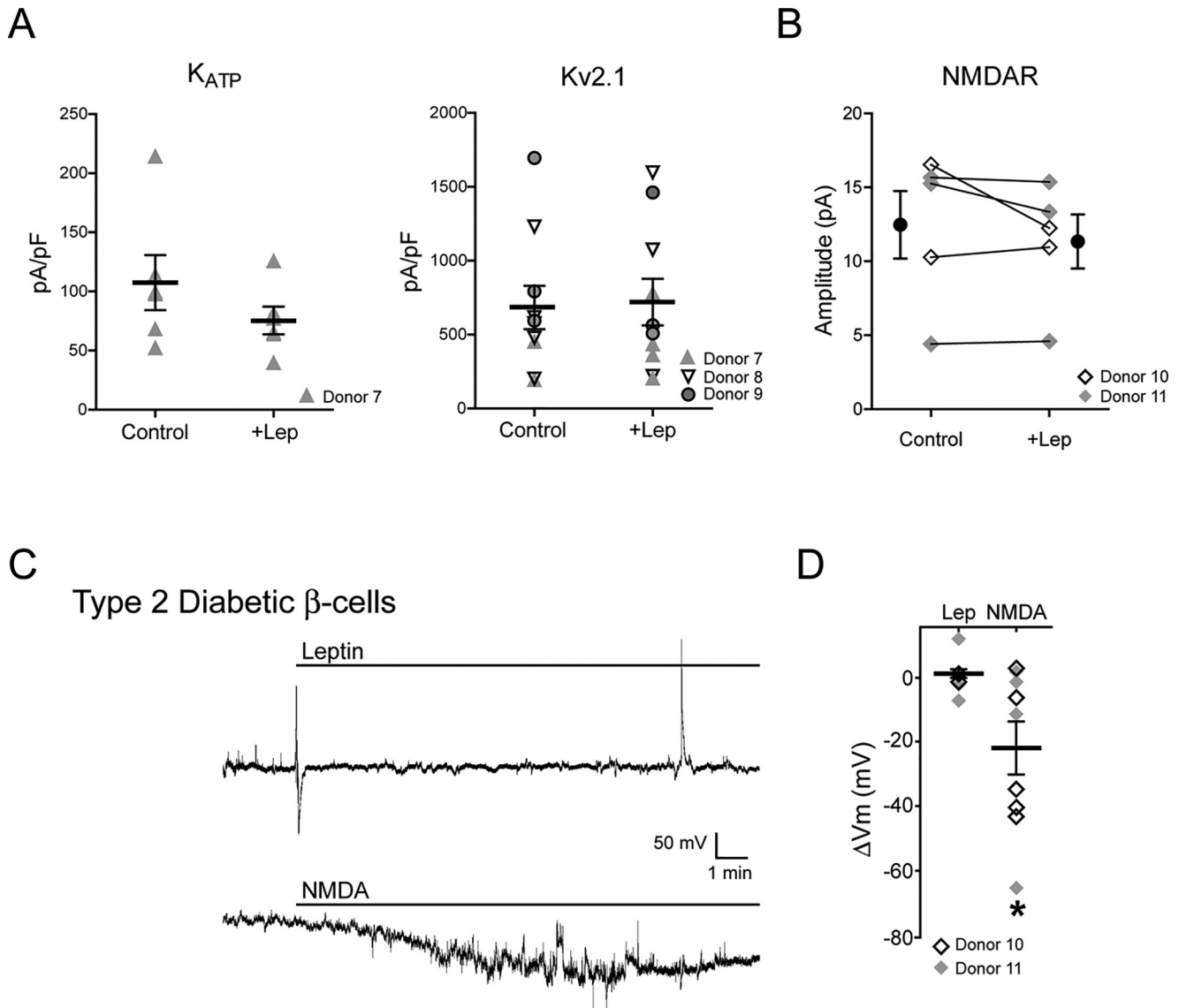


Figure 8. β -Cells from obese type 2 diabetic human donors failed to respond to leptin but retained response to NMDA. *A*, current density of K_{ATP} channels (*left*) and $Kv2.1$ channels (*right*) in β -cells from human diabetic donors treated with vehicle or 10 nM leptin (30 min). Different symbols are used to denote different donors. There is no statistically significant difference between leptin-treated and control groups. *B*, whole-cell NMDA currents in β -cells from diabetic donors before leptin application (control) or after 5-min incubation in 10 nM leptin (leptin). The mean (filled circles) and individual cell currents (before and after leptin treatment connected by a solid line) are shown. The open and filled gray diamonds represent different donors. *C*, representative cell-attached current-clamp recordings from human diabetic β -cells treated with 10 nM leptin (*top*) or 50 μ M NMDA (*bottom*). Note the spike in the top trace near the end of the recording is a solution suction artifact. *D*, group data showing membrane potential response to leptin or NMDA in β -cells isolated from human diabetic donors. *, $p < 0.05$, unpaired Student's t test compared with the leptin-treated group. Error bars, S.E.

sites, specifically Tyr-1292 and Tyr-1387, located in the C terminus of GluN2A prevented leptin-induced hyperpolarization. It is worth noting that Src has many downstream targets. For example, Src has been shown to regulate $Kv2.1$ activity (51) and actin dynamics (52, 53). Therefore, results from experiments involving pharmacological or molecular manipulation of Src activity could be due to Src regulation of other targets in addition to phosphorylation of NMDARs and downstream trafficking of K_{ATP} and $Kv2.1$ channels. Nonetheless, the collective evidence presented in this study together with our previously published studies (7, 9, 19) points to a signaling pathway in which leptin activates Src kinase to phosphorylate GluN2A of NMDARs, which leads to potentiation of NMDAR currents and increased Ca^{2+} influx. The increased Ca^{2+} influx

then activates $CaMKK\beta$ and AMPK, resulting in PKA-dependent actin depolymerization and trafficking of K_{ATP} and $Kv2.1$ channels to the cell surface, which culminates in hyperpolarization of β -cell membrane potential and reduced insulin secretion. Given Ca^{2+} influx is normally associated with β -cell depolarization and insulin secretion, it is likely that the Ca^{2+} influx through NMDARs triggered by leptin is localized and specifically coupled to downstream events that regulate potassium channel trafficking and hyperpolarize the membrane. Importantly, we demonstrate in β -cells from mice deficient in leptin signaling and obese diabetic human donors that direct activation of NMDARs by NMDA can bypass leptin resistance and induce membrane hyperpolarization, suggesting that the signaling pathway downstream of Src kinase modulation of

NMDARs remains operational and may be targeted to modulate insulin secretion.

Mechanism of NMDAR potentiation by leptin

NMDARs are allosterically modulated by a variety of endogenous extracellular ions. For example, Mg^{2+} can bind within the pore region of NMDAR and cause a voltage-dependent block (20). In addition, Zn^{2+} can promote voltage-dependent and voltage-independent inhibition of NMDAR activity (54–56). Voltage-dependent inhibition, like that observed with Mg^{2+} , occurs at a low-affinity GluN1 Zn^{2+} -binding site located within the channel pore (56), whereas voltage-independent inhibition appears to be mediated by a high-affinity Zn^{2+} -binding site located outside the channel pore and is associated with GluN2 subunits (57). Of the GluN2 subunits, GluN2A is 200-fold more sensitive to Zn^{2+} than GluN2B (58, 59). The binding of Zn^{2+} to these subunits is thought to trap the receptor in a low open probability state, reducing their activity (54, 55). Zn^{2+} has been shown to be co-released with several transmitters, including glutamate, and at some glutamatergic synapses within the brain, vesicular Zn^{2+} is thought to diminish NMDAR activity (60). Interestingly, β -cells contain and release high levels of Zn^{2+} due to its role in the biosynthesis and packaging of insulin (61). We speculate that NMDARs residing on the β -cell membrane would be subjected to high concentrations of Zn^{2+} inhibition during bouts of insulin secretion. Of note, phosphorylation of GluN2A by Src has been shown to potentiate NMDAR currents by reducing tonic inhibition of the receptor by Zn^{2+} (23, 25). A possible scenario is that under high glucose concentrations when β -cells are depolarized to relieve external Mg^{2+} block, NMDAR activity is still limited by Zn^{2+} co-released with insulin. However, inhibition by Zn^{2+} could be reduced by phosphorylating GluN2A via leptin-induced Src activation to regulate K_{ATP} and Kv2.1 surface expression and tune insulin secretion. In this way, GluN2A phosphorylation affords a mechanism to allow modulation of β -cell response to glucose stimulation by additional inputs such as leptin. Interestingly, in cells overexpressing GluN2A phosphomutants that failed to respond to leptin, bath application of 50 μM NMDA still induced membrane hyperpolarization. This suggests that NMDAR currents activated by endogenously released ligands and potentiated by leptin represent a fraction of total NMDAR currents that were activated by 50 μM NMDA under our experimental conditions.

Mechanism of Src activation by leptin

Expression of ObRb mRNAs in β -cells has been well-documented (1, 6, 62–65). It is assumed that leptin binds to ObRb expressed by pancreatic β -cells to suppress glucose-stimulated insulin secretion. However, leptin has also been reported to transactivate other cytokine receptor signaling molecules, including epidermal growth factor receptor, type 1 insulin-like growth factor receptor, low-density lipoprotein receptor-related protein, and vascular endothelial growth factor receptor (13). Our finding that *db/db* β -cells lack leptin-induced hyperpolarization lends strong support to the requirement of ObRb for leptin regulation of K^+ channel trafficking. The mechanism

by which ObRb activation leads to Src activation in β -cells awaits further investigation. The enzymatic activity of Src is tightly regulated by tyrosine phosphorylation at Tyr-418 in the catalytic domain and Tyr-529 at its C-terminal tail. When Tyr-529 is phosphorylated, the C-terminal tail acts as an autoinhibitory peptide to block kinase activity, and its dephosphorylation relieves autoinhibition, leading to autophosphorylation of Tyr-418, which further activates the kinase (38). Activation of ObRb is known to activate several tyrosine phosphatases, such as Shp2, which could dephosphorylate pY529 to activate the kinase (13, 38). Alternatively, direct recruitment of Src via the kinase's Src homology domains to phosphotyrosine in the activated leptin receptor complex or regulation by other kinases activated by leptin are also possibilities (38).

Tyrosine phosphorylation sites in GluN2A and GluN2B have been extensively investigated in recombinant expression systems and in neurons. The three GluN2A tyrosine residues examined in our study have all been shown to contribute to NMDAR current modulation (24, 25, 43). It is interesting that our data suggest that phosphorylation of Tyr-1292 and Y1387F but not Tyr-1325 are important for leptin response. This is in contrast to previous findings in the striatum neurons that Tyr-1325 is critical for Src-induced increase of NMDAR activity to regulate depression-related behavior (43). Very recently, Bland *et al.* (66) showed that leptin controls glutamatergic synaptogenesis and NMDAR trafficking via GluN2B phosphorylation by Fyn. Thus, the precise mechanisms and consequences of NMDAR modulation by leptin and SFKs are likely to be cell context-dependent.

Implications for leptin resistance and type 2 diabetes

We find that β -cells from obese type 2 diabetic human donors no longer hyperpolarize in response to leptin, as was also seen in β -cells from leptin-resistant, obese diabetic *db/db* mice. Examination of K_{ATP} and Kv2.1 currents confirms that the lack of hyperpolarization is due to the lack of increase in trafficking of these channels to the cell surface, indicating that leptin signaling was disrupted. Interestingly, we found that NMDAR current density was similar in β -cells from normal and obese diabetic donors with detectable currents (12.26 ± 4.12 pA/pF from normal donors, $n = 16$ (total of 35 cells from five donors (Table 1); 19 cells had no detectable currents) versus 11.60 ± 2.17 pA/pF from obese diabetic donors, $n = 20$ (total of 26 cells from two donors (Table 1); 6 cells had no detectable currents). Moreover, direct activation of NMDAR by NMDA triggered membrane hyperpolarization in both *db/db* β -cells and β -cells from human diabetic donors. Thus, despite leptin resistance, signaling mechanisms downstream of NMDARs (*i.e.* activation of CaMKK β , AMPK, and PKA-dependent actin depolymerization we reported previously (7, 9, 19)) remain functional to promote K_{ATP} and Kv2.1 channel trafficking to modulate β -cell excitability. The ability of leptin to temper glucose-stimulated insulin secretion has been proposed as part of an adipoinsular feedback loop between adipocytes and β -cells to prevent excessive secretion of insulin, an adipogenic hormone, thereby limiting fat mass (67). Disruption of leptin signaling in

Leptin and GluN2A phosphorylation in β -cells

β -cells has been shown to disrupt glucose homeostasis in some animal models (64, 65), although others argue against a major role of β -cell leptin signaling in glucose homeostasis (68). Whether the controversial findings were due to different mouse strains and genetic models used (69) remains to be resolved. Nonetheless, it is tempting to speculate on the potential of exploiting the leptin signaling pathway we have identified for the prevention and treatment of obesity-associated type 2 diabetes. In obese individuals, hyperleptinemia may result in leptin resistance (49, 70), which may lead to excessive insulin secretion. Hyperinsulinemia can then cause insulin resistance and hyperglycemia, further fueling obesity, leading to a loss of glucose control and eventually β -cell failure as seen in type 2 diabetes (71). Based on our finding that obese diabetic human β -cells, despite not being able to respond to leptin, retain response to NMDAR activation, stimulating NMDAR in leptin-resistant obese, prediabetic individuals may help to prevent excessive insulin secretion and thereby prevent or slow the development of type 2 diabetes (71). On the other hand, inhibition of NMDARs in individuals who have already developed type 2 diabetes may stimulate insulin secretion and alleviate hyperglycemia, as has been reported by Marquard *et al.* (17).

In summary, the current study identifies a novel leptin-signaling mechanism in β -cells wherein leptin activates Src kinase to phosphorylate GluN2A-containing NMDARs and potentiate NMDAR activity, thereby reducing β -cell excitability and insulin secretion. The findings build on our previously identified signaling pathway and provide a molecular explanation for the action of leptin. Moreover, they raise the therapeutic potential of targeting the pathway for the prevention and treatment of type 2 diabetes.

Experimental procedures

Chemicals

Leptin was purchased from Sigma. NMDA, diazoxide, roscovitine, Ro 25-6981, and TCN201 were purchased from Tocris Bioscience (Bristol, UK). AZD0530, GO6983, and dasatinib were from Selleckchem (Houston, TX, USA). Src kinase activator peptide (YEEI) was purchased from Santa Cruz Biotechnology, Inc. (Dallas, TX, USA).

INS-1 832/13 cell culture and transfection

INS-1 832/13 cells were cultured in RPMI 1640 medium (Invitrogen) supplemented with 10% fetal bovine serum (FBS), 100 units/ml penicillin, 100 μ g/ml streptomycin, 10 mM HEPES, 2 mM glutamine, 1 mM sodium pyruvate, and 50 μ M β -mercaptoethanol. Only cells within passage number 75 were used for experiments. For experiments involving transfection, cells were prepared as follows. INS-1 832/13 cells were grown on coverslips placed within 35-mm dishes and were transfected with WT (Addgene plasmid 45445), single GluN2A phosphorylation mutants (GluN2A^{Y1292F}, GluN2A^{Y1325F}, and GluN2A^{Y1387F}) or a triple phosphorylation mutant (GluN2A^{Y1292F,Y1325F,Y1387F}) using Lipofectamine 2000 (Invitrogen). Plasmids also encoded enhanced GFP at the N terminus to visually discern transfected from nontrans-

fected cells at time of recording 48–72 h after transfection. The kinase-dead Src mutant (pLNCX chick src K295R, a gift from Joan Brugge, Addgene plasmid 13659) transfection was carried out in 10-cm plates (cell confluence, ~50–60%) using Lipofectamine 2000 (20 μ g of DNA and 40 μ l of lipofectamine 2000) 48 h prior to experiments.

Dissociation of human pancreatic β -cells

Human β -cells were dissociated from human islets obtained through the Integrated Islets Distribution Program, as described previously (7, 9, 19). Briefly, human islets were cultured in RPMI 1640 medium with 10% FBS and 1% L-glutamine. For recording, islets were dissociated into single cells by trituration in a solution containing 116 mM NaCl, 5.5 mM D-glucose, 3 mM EGTA, and 0.1% BSA, pH 7.4. Dissociated cells were then plated on 0.1% gelatin-coated coverslips placed in 35-mm culture dishes (Falcon 35-3002). For electrophysiological experiments, β -cells were initially identified using the high autofluorescence signature of β -cells to 488-nm excitation, as these cells have high concentrations of unbound flavin adenine dinucleotide (72, 73). Dithizone (Sigma–Aldrich) staining was then used to further confirm β -cell identity at the end of each recording (74). Donor information for specific experiments is provided in Table 1.

Dissociation of mouse pancreatic β -cells

Mice were purchased from the Jackson Laboratory (Bar Harbor, ME, USA): control (C57BL/6J) and *db/db* [B6.BKS(D)-Lepr^{db/J}]. Pancreatic islets were isolated from the mice as described previously (75) and were performed in compliance with institutional guidelines and approved by the Oregon Health and Science University Animal Care and Use Committee. Following isolation, islets were cultured overnight in FBS-supplemented RPMI 1640 medium at 37 °C and 5% CO₂. Pancreatic β -cells were dissociated from islets using Spinners/EGTA solution (116 mM NaCl, 5.37 mM KCl, 0.8 mM MgSO₄, 26 mM NaHCO₃, 11.67 mM NaH₂PO₄, 5.5 mM D-glucose, 3 mM EGTA, 1% BSA, 1% phenol red (pH 7.4)). Islets were incubated twice in Spinners/EGTA for 10 min with slight agitation every 5 min. In between incubations with Spinners/EGTA, the islets were washed with FBS-supplemented RPMI 1640 medium. Dissociated cells were plated on glass coverslips coated with 1% gelatin (Sigma–Aldrich) and cultured overnight. The identity of individual β -cells was confirmed by dithizone staining at the end of each experiment (74).

RT-PCR

Total RNA was isolated from mouse brain and INS-1 832/13 cells using an RNeasy minikit (Qiagen, Hilden, Germany), and RT-PCR (from 1 μ g of mouse brain RNA and 1.8 μ g of INS-1 832/13 RNA) was performed using the Superscript RT-PCR system (Invitrogen) to examine the mRNA expression of NMDA receptor subunits, *Grin1* and *Grin2a–2d*. β -Actin mRNA was used as a standard reference housekeeping gene. The primers used were as follows: *Grin1*, 5'-GGTTTG-AGATGATGCGAGTCTAC (forward) and 5'-CAGC-AGAGCCGTCACATTCCTTGG (reverse); *Grin2a*, 5'-

CAATCTGACTGGATCACAGAGC (forward) and 5'-CTGTCCTTCCCTTGAAAGGATC (reverse); *Grin2b*, 5'-CAA-TAACCCACCCTGTGAGG (forward) and 5'-GGTGGGTTGTCACAGTCATAG (reverse); *Grin2c*, 5'-ACATGAAGTATC-CAGTATGG (forward) and 5'-GTTCTGGTTGTAGCTGACAG (reverse); *Grin2d*, 5'-AGGTGTTCTATCAGCGTG (forward) and 5'-TGTAGCTGTGCATGTCAG (reverse); and β -actin, 5'-CGTAAAGACCTCTATGCCAA (forward) and 5'-AGCCATGCCAAATGTGTCAT (reverse).

Immunoblotting

INS-1 832/13 cells were lysed in lysis buffer (50 mM Tris-HCl, 2 mM EDTA, 2 mM EGTA, 100 mM NaCl, 1% Triton X-100, pH 7.4, with cOmplete EDTA-free protease inhibitor mixture (Roche, Basel, Switzerland) and Halt-phosphatase inhibitor mixture (Thermo Scientific) for 30 min at 4 °C, and cell lysates were cleared by centrifugation (MIKRO 200R, Helmer Scientific, Noblesville, IN, USA) at 14,000 rpm for 10 min at 4 °C. In some experiments, lysis buffer was replaced with ice-cold PBS to aid in the isolation of membrane proteins. PBS cell lysates were briefly spun at 3000 rpm for 5 min at 4 °C, and the membrane pellet was homogenized in a hypotonic solution containing 15 mM KCl, 10 mM HEPES, 1.5 mM MgCl₂ with phosphatase and protease inhibitors by passing 30 times through a 27½ gauge needle. Spun at 6,000 rpm at 4 °C for 2 min to remove nuclei and cellular debris. Supernatant was collected and transferred to 1.5-ml Beckman centrifuge tubes and spun at 54,000 rpm at 4 °C for 60 min. The resulting membrane pellet was resuspended in solubilization buffer containing 0.2 M NaCl, 0.1 M KCl, 0.05 M HEPES, and proteins were separated by SDS-PAGE (7.5% polyacrylamide gel) and transferred onto polyvinylidene difluoride membranes (Millipore, Burlington, MA, USA). Membranes were incubated overnight at 4 °C with primary antibody diluted in TBST (TBS plus 0.1% Tween 20) followed by incubation with horseradish peroxidase-conjugated secondary antibodies in TBST for 1 h at room temperature. Primary antibodies used were anti-phosphorylated Src^{Y418} (human Src numbering; rabbit monoclonal; Abcam, ab133460; 1:1000 dilution), anti-c-Src; Abcam, ab16885; 1:100 dilution), anti-GluN1 (NeuroMab, 75-272; 1:1000 dilution), anti-GluN2A (NeuroMab, 75-288; 1:1000 dilution), and anti-GluN2B (NeuroMab, 75-101; 1:1000 dilution). Blots were developed using Super Signal West Femto (Pierce) and imaged with FluorChemE (ProteinSimple, San Jose, CA, USA), protein bands were quantified using ImageJ (National Institutes of Health) and normalized to the corresponding controls.

Immunocytochemistry

INS-1 832/13 cells were fixed in 2% paraformaldehyde in PBS for 10 min at room temperature, permeabilized with 0.2% Triton X-100 in 1% BSA/PBS, and blocked for 60 min with 1% BSA in PBST (PBS + 0.1% Tween 20) before being incubated overnight at 4 °C with primary rabbit polyclonal antibodies directed against phospho-Src^{Y418} (Abcam, ab4816). Proteins were visualized using Alexa 488-conjugated secondary antibodies. Fluorescent images were acquired using a Zeiss LSM780 confocal microscope equipped with a ×63 oil immersion objec-

tive. Images were processed and analyzed using NIH ImageJ software (76). For surface staining of GFP-GluN2A^{WT} and GFP-GluN2A^{Y1292E,Y1325E,Y1387F}, cells were incubated in cold DPBS containing anti-GFP antibody (1:100; ThermoScientific, G10362) at 4 °C for 30 min. Cells were then fixed as described above, and surface GFP was visualized using a Cy3-conjugated secondary antibody.

Immunoprecipitation

48 h post-transfection of GFP-GluN2A^{WT}, cells were collected in DPBS. A membrane pellet was obtained following the protocol described above. The pellet was then solubilized in co-immunoprecipitation buffer (0.5 mM Tris-HCl, 150 mM NaCl, 0.5% Igepal, pH 7.2) and incubated with 25 μ l of GFP-Trap Dynabeads (Chromotek) overnight at 4 °C. The beads were washed twice with co-immunoprecipitation buffer. Proteins bound to the beads were then eluted in 2× protein loading buffer for 10 min at 95 °C. Samples were analyzed via immunoblotting for GFP (1:100; ThermoScientific, G10362), GluN2A (1:1000; NeuroMab, 75-288), and GluN1 (1:1000; NeuroMab, 75-272) and simultaneously imaged using near-IR secondary antibodies (LI-COR IRDye).

Surface biotinylation

INS-1 832/13 cells were incubated in RPMI 1640 for 1 h at 37 °C prior to a 30-min treatment with vehicle or leptin (10 nM). Cells were then washed four times with cold DPBS and incubated with 1 mg/ml EZ-Link Sulfo-NHS-SS-Biotin (Pierce) in DPBS with vehicle or leptin for 30 min at 4 °C. The reaction was terminated by incubating cells twice for 5 min with DPBS containing 50 mM glycine followed by two washes with cold DPBS. Cells were then lysed in 300 μ l of lysis buffer as described above, and 500 μ g of total lysate was incubated with 50 μ l of a 50% slurry of NeutraAvidin-agarose beads (Pierce) overnight at 4 °C. Biotinylated proteins were eluted with 2× protein loading buffer for 15 min at 37 °C. Both eluent and input samples (50 μ g of total cell lysate) were analyzed by immunoblotting using anti-SUR1 antibody (raised against a hamster SUR1 C-terminal peptide KDSVFASFVRADK) as described previously (7).

Electrophysiology

Electrophysiological recordings were conducted using an Axon 200B amplifier (Molecular Devices, Sunnyvale, CA, USA) with Clampex 9.2 (pCLAMP) software. Signals were acquired at 20 kHz and filtered at 2 kHz. Recording electrodes (tip resistances ranged between 3 and 6 megaohms) were pulled from nonheparinized Kimble glass (Thermo Fisher Scientific, Waltham, MA, USA) using a P-97 micropipette puller (Sutter Instruments). For whole-cell recording of NMDA currents, external Tyrode's solution contained 137 mM NaCl, 5.4 mM KCl, 1.8 mM CaCl₂, 0.5 mM MgCl₂, 5 mM Na-HEPES, 3 mM NaHCO₃, and 0.16 mM NaH₂PO₄ (pH 7.2). The external solution was supplemented with 0.1 mM glycine and 11 mM glucose, and in some experiments Mg²⁺ was omitted as specified in the figure legends. The internal pipette solution contained 140 mM potassium gluconate, 6 mM EGTA, 10 mM HEPES, 5 mM

Leptin and GluN2A phosphorylation in β -cells

K₂ATP, 1 mM CaCl₂ (pH 7.2). To induce NMDA-mediated currents, cells were held at -70 mV, and NMDA (1 mM) was puffed (3–5 p.s.i. for 0.5 s) with carbogen using 1–0.5-megaohm micropipettes connected to a Multi-function Microforge Controller DMF1000 (World Precision Instruments, Sarasota, FL, USA) equipped with a pressure regulator. In experiments measuring NMDAR current response to Mg²⁺ block (Fig. 1B), leptin (Figs. 3 and 8B), and leptin plus AZD (Fig. 3), 1 mM NMDA was puffed repeatedly at 1-min intervals 3–5 times to establish control baseline. Only cells that showed reproducible currents to repeated NMDA puffs during control baseline measurements were subsequently treated with 100 μ M Mg²⁺, 10 nM leptin, or leptin plus AZD for 5 min, after which 1 mM NMDA was again puffed at 1-min intervals 3–5 times. The currents before and after treatments were then averaged, and the averaged values are shown as individual data points in the figures.

Whole-cell K_{ATP} and Kv2.1 current recordings (Fig. 8A) were conducted as described previously (7, 9). For K_{ATP} currents, cells were held at -70 mV, and K_{ATP} currents were recorded at two voltage steps (-50 and -90 mV) applied every 2 s. Pipette solution contained 140 mM KCl, 10 mM K-HEPES, 1 mM K-EGTA, pH 7.3. The bath solution contained 137 mM NaCl, 5.4 mM KCl, 1.8 mM CaCl₂, 0.5 mM MgCl₂, 5 mM Na-HEPES, 3 mM NHCO₃, 0.16 mM NaH₂PO₄, pH 7.2. Diazoxide (200 μ M) was applied to the bath solution immediately after break-in to maximally stimulate K_{ATP} channels. After the current had plateaued, 300 μ M tolbutamide (a K_{ATP} channel inhibitor) was applied, and residual currents were subtracted from maximal currents observed in diazoxide and divided by cell capacitance to obtain K_{ATP} current density. For Kv2.1, micropipettes were filled with an internal solution containing 140 mM KCl, 1 mM CaCl₂, 2 mM MgCl₂, 5 mM EGTA, 5 mM ATP, 10 mM glucose, and 10 mM HEPES, pH 7.3. The bath solution contained the following: 140 mM NaCl, 5 mM KCl, 4 mM MgCl₂, 11 mM glucose, 10 mM HEPES, pH 7.3. Ca²⁺ was excluded from the bath solution to eliminate calcium channel currents. A 30-ms prepulse to -10 mV was used to inactivate transient potassium channel currents and voltage-dependent Na⁺ currents. The sustained current at $+80$ mV, after subtracting currents remaining in a 10 mM concentration of the potassium current blocker tetraethylammonium, was divided by cell capacitance for Kv2.1 current density calculation.

For cell-attached recording to monitor membrane potentials, micropipettes were filled with 140 mM NaCl. The bath solution contained 137 mM NaCl, 5.4 mM KCl, 1.8 mM CaCl₂, 0.5 mM MgCl₂, 5 mM Na-HEPES, 3 mM NHCO₃, 0.16 mM NaH₂PO₄, 11 mM glucose, pH 7.2. The liquid junction potential was measured to be -10 mV and corrected from the recorded V_m . Seal resistances between the recording pipette and the cell membrane ranged between 4 and 11 gigaohms, and membrane potentials were monitored in current-clamp mode ($I = 0$). After correction for the liquid junction potential, the average starting V_m was around -4 mV. Note that the V_m estimated in this configuration depends on the ratio of the seal resistance and the combined patch and cell resistance, where the ratio of recorded V_m and true membrane potential = $(R_{\text{seal}}/R_{\text{patch}} + R_{\text{cell}})/(1 + (R_{\text{seal}}/R_{\text{patch}} + R_{\text{cell}}))$ (32). As such, the recorded V_m is an under-

estimate of the actual membrane potential (*i.e.* more depolarized than the actual V_m) (31, 32). Because the recorded V_m under this configuration is only a proxy of the true membrane potential, we only used it to track changes in membrane potential (31, 32). Seal resistance was monitored before and after the recording, and only cells that showed stable baseline membrane potential prior to leptin/drug application and that maintained good seal resistance were included for analysis. In addition, the K_{ATP} channel opener diazoxide or inhibitor tolbutamide was used when applicable to ensure cell and patch integrity as we reported previously (19) and in the current study (see Figs. 4 and 7). For whole-cell current-clamp recordings of membrane potential (Fig. 2, C and D), pipette solution contained 130 mM potassium gluconate, 10 mM KCl, 10 mM HEPES, 6 mM EGTA, 0.1 mM CaCl₂, 1 mM MgCl₂, and 5 mM ATP, with or without the SF activator YEEI phosphopeptide (EPQpYEEIPIYL at 1 μ M). All recordings were analyzed using Clampfit 9.2 (pCLAMP).

Statistical analysis

Results are expressed as mean \pm S.E. One-way analysis of variance with a post hoc Dunnett's test (Fig. 5E) or Friedman's test (Fig. 3B) was used for multiple comparisons where different experimental conditions were carried out side by side. For most experiments, difference between control and treated groups was tested using a paired *t* test or unpaired *t* tests (for comparable sample sizes) or Welch's *t* test (for significantly unequal sample sizes in Fig. 6D) as detailed in the figure legends. The level of statistical significance was set at $p < 0.05$.

Data availability

All data are contained in the article.

Acknowledgments—We thank Dr. Christopher Newgard for the rat insulinoma INS-1 clone 832/13 cells.

Author contributions—V. A. C., Y. W., D. A. F., and S.-L. S. conceptualization; V. A. C., Y. W., D. A. F., and S.-L. S. data curation; V. A. C., Y. W., D. A. F., and S.-L. S. formal analysis; V. A. C., Y. W., Z. Y., A. E., J. D., and D. A. F. investigation; V. A. C., A. E., P. K., D. A. F., and S.-L. S. writing-review and editing; Y. W., D. A. F., and S.-L. S. writing-original draft; S.-L. S. funding acquisition; S.-L. S. project administration.

Funding and additional information—This work was supported by National Institutes of Health Grants R01DK057699 and 3R01DK057699-14S1 (to S.-L. S.). P. K. was supported by National Institutes of Health Grant P51 OD011092 (to the Oregon National Primate Research Center). The content is solely the responsibility of the authors and does not necessarily represent the official views of the National Institutes of Health.

Conflict of interest—The authors declare that they have no conflicts of interest with the contents of this article.

Abbreviations—The abbreviations used are: AMPK, AMP-activated protein kinase; SFK, Src family kinase; NMDA, *N*-methyl-D-

aspartate; NMDAR, NMDA receptor; CaMKK β , calcium/calmodulin-dependent protein kinase kinase β ; PKA, protein kinase A; PKC, protein kinase C; AZD, AZD0530; IIDP, Integrated Islets Distribution Program; pF, picofarads; FBS, fetal bovine serum; DPBS, Dulbecco's PBS.

References

- Emilsson, V., Liu, Y. L., Cawthorne, M. A., Morton, N. M., and Davenport, M. (1997) Expression of the functional leptin receptor mRNA in pancreatic islets and direct inhibitory action of leptin on insulin secretion. *Diabetes* **46**, 313–316 [CrossRef Medline](#)
- Fehmann, H. C., Peiser, C., Bode, H. P., Stamm, M., Staats, P., Hedetoft, C., Lang, R. E., and Göke, B. (1997) Leptin: a potent inhibitor of insulin secretion. *Peptides* **18**, 1267–1273 [CrossRef Medline](#)
- Kieffer, T. J., Heller, R. S., Leech, C. A., Holz, G. G., and Habener, J. F. (1997) Leptin suppression of insulin secretion by the activation of ATP-sensitive K⁺ channels in pancreatic beta-cells. *Diabetes* **46**, 1087–1093 [CrossRef Medline](#)
- Kulkarni, R. N., Wang, Z. L., Wang, R. M., Hurley, J. D., Smith, D. M., Ghaitei, M. A., Withers, D. J., Gardiner, J. V., Bailey, C. J., and Bloom, S. R. (1997) Leptin rapidly suppresses insulin release from insulinoma cells, rat and human islets and, in vivo, in mice. *J. Clin. Invest.* **100**, 2729–2736 [CrossRef Medline](#)
- Ookuma, M., Ookuma, K., and York, D. A. (1998) Effects of leptin on insulin secretion from isolated rat pancreatic islets. *Diabetes* **47**, 219–223 [CrossRef Medline](#)
- Poitout, V., Rouault, C., Guerre-Millo, M., Briaud, I., and Reach, G. (1998) Inhibition of insulin secretion by leptin in normal rodent islets of Langerhans. *Endocrinology* **139**, 822–826 [CrossRef Medline](#)
- Chen, P. C., Kryukova, Y. N., and Shyng, S. L. (2013) Leptin regulates KATP channel trafficking in pancreatic β -cells by a signaling mechanism involving AMP-activated protein kinase (AMPK) and cAMP-dependent protein kinase (PKA). *J. Biol. Chem.* **288**, 34098–34109 [CrossRef Medline](#)
- Park, S. H., Ryu, S. Y., Yu, W. J., Han, Y. E., Ji, Y. S., Oh, K., Sohn, J. W., Lim, A., Jeon, J. P., Lee, H., Lee, K. H., Lee, S. H., Berggren, P. O., Jeon, J. H., and Ho, W. K. (2013) Leptin promotes K_{ATP} channel trafficking by AMPK signaling in pancreatic β -cells. *Proc. Natl. Acad. Sci. U. S. A.* **110**, 12673–12678 [CrossRef Medline](#)
- Wu, Y., Shyng, S. L., and Chen, P. C. (2015) Concerted trafficking regulation of Kv2.1 and KATP channels by leptin in pancreatic β -cells. *J. Biol. Chem.* **290**, 29676–29690 [CrossRef Medline](#)
- Jacobson, D. A., and Shyng, S. L. (2020) Ion channels of the islets in type 2 diabetes. *J. Mol. Biol.* **432**, 1326–1346 [CrossRef Medline](#)
- Rorsman, P., and Ashcroft, F. M. (2018) Pancreatic β -cell electrical activity and insulin secretion: of mice and men. *Physiol. Rev.* **98**, 117–214 [CrossRef Medline](#)
- Friedman, J. (2016) The long road to leptin. *J. Clin. Invest.* **126**, 4727–4734 [CrossRef Medline](#)
- Wautman, J., Zabeau, L., and Tavernier, J. (2017) The leptin receptor complex: heavier than expected? *Front. Endocrinol. (Lausanne)* **8**, 30 [CrossRef Medline](#)
- Jiang, L., Li, Z., and Rui, L. (2008) Leptin stimulates both JAK2-dependent and JAK2-independent signaling pathways. *J. Biol. Chem.* **283**, 28066–28073 [CrossRef Medline](#)
- Cochrane, V., and Shyng, S. L. (2019) Leptin-induced trafficking of K_{ATP} channels: a mechanism to regulate pancreatic beta-cell excitability and insulin secretion. *Int. J. Mol. Sci.* **20**, 2660 [CrossRef Medline](#)
- Paoletti, P., Bellone, C., and Zhou, Q. (2013) NMDA receptor subunit diversity: impact on receptor properties, synaptic plasticity and disease. *Nat. Rev. Neurosci.* **14**, 383–400 [CrossRef Medline](#)
- Marquard, J., Otter, S., Welters, A., Stirban, A., Fischer, A., Eglinger, J., Herebian, D., Kletke, O., Klemen, M. S., Stožer, A., Wnendt, S., Piemonti, L., Köhler, M., Ferrer, J., Thorens, B., et al. (2015) Characterization of pancreatic NMDA receptors as possible drug targets for diabetes treatment. *Nat. Med.* **21**, 363–372 [CrossRef Medline](#)
- Otter, S., and Lammert, E. (2016) Exciting times for pancreatic islets: glutamate signaling in endocrine cells. *Trends Endocrinol. Metab.* **27**, 177–188 [CrossRef Medline](#)
- Wu, Y., Fortin, D. A., Cochrane, V. A., Chen, P. C., and Shyng, S. L. (2017) NMDA receptors mediate leptin signaling and regulate potassium channel trafficking in pancreatic β -cells. *J. Biol. Chem.* **292**, 15512–15524 [CrossRef Medline](#)
- Hansen, K. B., Yi, F., Perszyk, R. E., Furukawa, H., Wollmuth, L. P., Gibb, A. J., and Traynelis, S. F. (2018) Structure, function, and allosteric modulation of NMDA receptors. *J. Gen. Physiol.* **150**, 1081–1105 [CrossRef Medline](#)
- Wrighton, D. C., Baker, E. J., Chen, P. E., and Wyllie, D. J. (2008) Mg²⁺ and memantine block of rat recombinant NMDA receptors containing chimeric NR2A/2D subunits expressed in *Xenopus laevis* oocytes. *J. Physiol.* **586**, 211–225 [CrossRef Medline](#)
- Chen, B. S., and Roche, K. W. (2007) Regulation of NMDA receptors by phosphorylation. *Neuropharmacology* **53**, 362–368 [CrossRef Medline](#)
- Salter, M. W., and Kalia, L. V. (2004) Src kinases: a hub for NMDA receptor regulation. *Nat. Rev. Neurosci.* **5**, 317–328 [CrossRef Medline](#)
- Yang, M., and Leonard, J. P. (2001) Identification of mouse NMDA receptor subunit NR2A C-terminal tyrosine sites phosphorylated by coexpression with v-Src. *J. Neurochem.* **77**, 580–588 [CrossRef Medline](#)
- Zheng, F., Gingrich, M. B., Traynelis, S. F., and Conn, P. J. (1998) Tyrosine kinase potentiates NMDA receptor currents by reducing tonic zinc inhibition. *Nat. Neurosci.* **1**, 185–191 [CrossRef Medline](#)
- Heida, N. M., Leifheit-Nestler, M., Schroeter, M. R., Müller, J. P., Cheng, I. F., Henkel, S., Limbourg, A., Limbourg, F. P., Alves, F., Quigley, J. P., Ruggeri, Z. M., Hasenfuss, G., Konstantinides, S., and Schäfer, K. (2010) Leptin enhances the potency of circulating angiogenic cells via Src kinase and integrin α v β 5: implications for angiogenesis in human obesity. *Arterioscler. Thromb. Vasc. Biol.* **30**, 200–206 [CrossRef Medline](#)
- Shanley, L. J., Irving, A. J., and Harvey, J. (2001) Leptin enhances NMDA receptor function and modulates hippocampal synaptic plasticity. *J. Neurosci.* **21**, RC186 [CrossRef Medline](#)
- Kuner, T., and Schoepfer, R. (1996) Multiple structural elements determine subunit specificity of Mg²⁺ block in NMDA receptor channels. *J. Neurosci.* **16**, 3549–3558 [CrossRef Medline](#)
- Stroebel, D., Casado, M., and Paoletti, P. (2018) Triheteromeric NMDA receptors: from structure to synaptic physiology. *Curr. Opin. Physiol.* **2**, 1–12 [CrossRef Medline](#)
- Edman, S., McKay, S., Macdonald, L. J., Samadi, M., Livesey, M. R., Hardingham, G. E., and Wyllie, D. J. (2012) TCN 201 selectively blocks GluN2A-containing NMDARs in a GluN1 co-agonist dependent but non-competitive manner. *Neuropharmacology* **63**, 441–449 [CrossRef Medline](#)
- Mason, M. J., Simpson, A. K., Mahaut-Smith, M. P., and Robinson, H. P. (2005) The interpretation of current-clamp recordings in the cell-attached patch-clamp configuration. *Biophys. J.* **88**, 739–750 [CrossRef Medline](#)
- Perkins, K. L. (2006) Cell-attached voltage-clamp and current-clamp recording and stimulation techniques in brain slices. *J. Neurosci. Methods* **154**, 1–18 [CrossRef Medline](#)
- Fischer, G., Mutel, V., Trube, G., Malherbe, P., Kew, J. N., Mohacsi, E., Heitz, M. P., and Kemp, J. A. (1997) Ro 25-6981, a highly potent and selective blocker of N-methyl-D-aspartate receptors containing the NR2B subunit. Characterization *in vitro*. *J. Pharmacol. Exp. Ther.* **283**, 1285–1292 [Medline](#)
- Yi, F., Mou, T. C., Dorsett, K. N., Volkman, R. A., Menniti, F. S., Sprang, S. R., and Hansen, K. B. (2016) Structural basis for negative allosteric modulation of GluN2A-containing NMDA receptors. *Neuron* **91**, 1316–1329 [CrossRef Medline](#)
- Grant, E. R., Guttman, R. P., Seifert, K. M., and Lynch, D. R. (2001) A region of the rat N-methyl-D-aspartate receptor 2A subunit that is sufficient for potentiation by phorbol esters. *Neurosci. Lett.* **310**, 9–12 [CrossRef Medline](#)
- Li, B. S., Sun, M. K., Zhang, L., Takahashi, S., Ma, W., Vinade, L., Kulkarni, A. B., Brady, R. O., and Pant, H. C. (2001) Regulation of NMDA receptors

Leptin and GluN2A phosphorylation in β -cells

- by cyclin-dependent kinase-5. *Proc. Natl. Acad. Sci. U. S. A.* **98**, 12742–12747 [CrossRef Medline](#)
37. Yang, K., Trepanier, C., Sidhu, B., Xie, Y. F., Li, H., Lei, G., Salter, M. W., Orser, B. A., Nakazawa, T., Yamamoto, T., Jackson, M. F., and Macdonald, J. F. (2012) Metaplasticity gated through differential regulation of GluN2A versus GluN2B receptors by Src family kinases. *EMBO J.* **31**, 805–816 [CrossRef Medline](#)
38. Roskoski, R., Jr (2015) Src protein-tyrosine kinase structure, mechanism, and small molecule inhibitors. *Pharmacol. Res.* **94**, 9–25 [CrossRef Medline](#)
39. Boggon, T. J., and Eck, M. J. (2004) Structure and regulation of Src family kinases. *Oncogene* **23**, 7918–7927 [CrossRef Medline](#)
40. Liu, X., Brodeur, S. R., Gish, G., Songyang, Z., Cantley, L. C., Laudano, A. P., and Pawson, T. (1993) Regulation of c-Src tyrosine kinase activity by the Src SH2 domain. *Oncogene* **8**, 1119–1126 [Medline](#)
41. Köhr, G., and Seeburg, P. H. (1996) Subtype-specific regulation of recombinant NMDA receptor-channels by protein tyrosine kinases of the Src family. *J. Physiol.* **492**, 445–452 [CrossRef Medline](#)
42. Wang, W. S., Chen, Z. G., Liu, W. T., Chi, Z. Q., He, L., and Liu, J. G. (2015) Dorsal hippocampal NMDA receptor blockade impairs extinction of naloxone-precipitated conditioned place aversion in acute morphine-treated rats by suppressing ERK and CREB phosphorylation in the basolateral amygdala. *Br. J. Pharmacol.* **172**, 482–491 [CrossRef Medline](#)
43. Taniguchi, S., Nakazawa, T., Tanimura, A., Kiyama, Y., Tezuka, T., Watabe, A. M., Katayama, N., Yokoyama, K., Inoue, T., Izumi-Nakaseko, H., Kakuta, S., Sudo, K., Iwakura, Y., Umemori, H., Inoue, T., *et al.* (2009) Involvement of NMDAR2A tyrosine phosphorylation in depression-related behaviour. *EMBO J.* **28**, 3717–3729 [CrossRef Medline](#)
44. Barria, A., and Malinow, R. (2002) Subunit-specific NMDA receptor trafficking to synapses. *Neuron* **35**, 345–353 [CrossRef Medline](#)
45. Roskoski, R., Jr. (2005) Src kinase regulation by phosphorylation and dephosphorylation. *Biochem. Biophys. Res. Commun.* **331**, 1–14 [CrossRef Medline](#)
46. Pucheta-Martinez, E., Saladino, G., Morando, M. A., Martinez-Torrecedrada, J., Lelli, M., Sutto, L., D'Amelio, N., and Gervasio, F. L. (2016) An allosteric cross-talk between the activation loop and the ATP binding site regulates the activation of Src kinase. *Sci. Rep.* **6**, 24235 [CrossRef Medline](#)
47. Yoder, S. M., Dineen, S. L., Wang, Z., and Thurmond, D. C. (2014) YES, a Src family kinase, is a proximal glucose-specific activator of cell division cycle control protein 42 (Cdc42) in pancreatic islet β cells. *J. Biol. Chem.* **289**, 11476–11487 [CrossRef Medline](#)
48. Socodato, R., Santiago, F. N., Portugal, C. C., Domith, I., Encarnaçao, T. G., Loiola, E. C., Ventura, A. L., Cossenza, M., Relvas, J. B., Castro, N. G., and Paes-de-Carvalho, R. (2017) Dopamine promotes NMDA receptor hypofunction in the retina through D1 receptor-mediated Csk activation, Src inhibition and decrease of GluN2B phosphorylation. *Sci. Rep.* **7**, 40912 [CrossRef Medline](#)
49. Konner, A. C., and Bruning, J. C. (2012) Selective insulin and leptin resistance in metabolic disorders. *Cell Metab.* **16**, 144–152 [CrossRef Medline](#)
50. Chen, H., Charlat, O., Tartaglia, L. A., Woolf, E. A., Weng, X., Ellis, S. J., Lakey, N. D., Culpepper, J., Moore, K. J., Breitbart, R. E., Duyk, G. M., Tepper, R. I., and Morgenstern, J. P. (1996) Evidence that the diabetes gene encodes the leptin receptor: identification of a mutation in the leptin receptor gene in db/db mice. *Cell* **84**, 491–495 [CrossRef Medline](#)
51. Song, M. Y., Hong, C., Bae, S. H., So, I., and Park, K. S. (2012) Dynamic modulation of the kv2.1 channel by SRC-dependent tyrosine phosphorylation. *J. Proteome Res.* **11**, 1018–1026 [CrossRef Medline](#)
52. Destaing, O., Sanjay, A., Itzstein, C., Horne, W. C., Toomre, D., De Camilli, P., and Baron, R. (2008) The tyrosine kinase activity of c-Src regulates actin dynamics and organization of podosomes in osteoclasts. *Mol. Biol. Cell* **19**, 394–404 [CrossRef Medline](#)
53. Olivares, M. J., González-Jamett, A. M., Guerra, M. J., Baez-Matus, X., Haro-Acuña, V., Martínez-Quiles, N., and Cardeñas, A. M. (2014) Src kinases regulate de novo actin polymerization during exocytosis in neuroendocrine chromaffin cells. *PLoS ONE* **9**, e99001 [CrossRef Medline](#)
54. Amico-Ruvio, S. A., Murthy, S. E., Smith, T. P., and Popescu, G. K. (2011) Zinc effects on NMDA receptor gating kinetics. *Biophys. J.* **100**, 1910–1918 [CrossRef Medline](#)
55. Dolino, D. M., Chatterjee, S., MacLean, D. M., Flatebo, C., Bishop, L. D. C., Shaikh, S. A., Landes, C. F., and Jayaraman, V. (2017) The structure-energy landscape of NMDA receptor gating. *Nat. Chem. Biol.* **13**, 1232–1238 [CrossRef Medline](#)
56. Jalali-Yazdi, F., Chowdhury, S., Yoshioka, C., and Gouaux, E. (2018) Mechanisms for zinc and proton inhibition of the GluN1/GluN2A NMDA receptor. *Cell* **175**, 1520–1532 [CrossRef Medline](#)
57. Fayyazuddin, A., Villarroel, A., Le Goff, A., Lerma, J., and Neyton, J. (2000) Four residues of the extracellular N-terminal domain of the NR2A subunit control high-affinity Zn²⁺ binding to NMDA receptors. *Neuron* **25**, 683–694 [CrossRef Medline](#)
58. Paoletti, P., Ascher, P., and Neyton, J. (1997) High-affinity zinc inhibition of NMDA NR1-NR2A receptors. *J. Neurosci.* **17**, 5711–5725 [CrossRef Medline](#)
59. Traynelis, S. F., Burgess, M. F., Zheng, F., Lyuboslavsky, P., and Powers, J. L. (1998) Control of voltage-independent zinc inhibition of NMDA receptors by the NR1 subunit. *J. Neurosci.* **18**, 6163–6175 [CrossRef Medline](#)
60. Vogt, K., Mellor, J., Tong, G., and Nicoll, R. (2000) The actions of synaptically released zinc at hippocampal mossy fiber synapses. *Neuron* **26**, 187–196 [CrossRef Medline](#)
61. Dodson, G., and Steiner, D. (1998) The role of assembly in insulin's biosynthesis. *Curr. Opin. Struct. Biol.* **8**, 189–194 [CrossRef Medline](#)
62. Kieffer, T. J., Heller, R. S., and Habener, J. F. (1996) Leptin receptors expressed on pancreatic beta-cells. *Biochem. Biophys. Res. Commun.* **224**, 522–527 [CrossRef Medline](#)
63. Seufert, J., Kieffer, T. J., Leech, C. A., Holz, G. G., Moritz, W., Ricordi, C., and Habener, J. F. (1999) Leptin suppression of insulin secretion and gene expression in human pancreatic islets: implications for the development of adipogenic diabetes mellitus. *J. Clin. Endocrinol. Metab.* **84**, 670–676 [CrossRef Medline](#)
64. Covey, S. D., Wideman, R. D., McDonald, C., Unniappan, S., Huynh, F., Asadi, A., Speck, M., Webber, T., Chua, S. C., and Kieffer, T. J. (2006) The pancreatic beta cell is a key site for mediating the effects of leptin on glucose homeostasis. *Cell Metab.* **4**, 291–302 [CrossRef Medline](#)
65. Morioka, T., Asilmaz, E., Hu, J., Dishinger, J. F., Kurpad, A. J., Elias, C. F., Li, H., Elmquist, J. K., Kennedy, R. T., and Kulkarni, R. N. (2007) Disruption of leptin receptor expression in the pancreas directly affects beta cell growth and function in mice. *J. Clin. Invest.* **117**, 2860–2868 [CrossRef Medline](#)
66. Bland, T., Zhu, M., Dillon, C., Sahin, G. S., Rodriguez-Llamas, J. L., Appleyard, S. M., and Wayman, G. A. (2020) Leptin controls glutamatergic synaptogenesis and NMDA-receptor trafficking via Fyn kinase regulation of NR2B. *Endocrinology* **161**, bqz030 [CrossRef](#)
67. Kieffer, T. J., and Habener, J. F. (2000) The adipoinular axis: effects of leptin on pancreatic beta-cells. *Am. J. Physiol. Endocrinol. Metab.* **278**, E1–E14 [CrossRef Medline](#)
68. Soedling, H., Hodson, D. J., Adrianssens, A. E., Gribble, F. M., Reimann, F., Trapp, S., and Rutter, G. A. (2015) Limited impact on glucose homeostasis of leptin receptor deletion from insulin- or proglucagon-expressing cells. *Mol. Metab.* **4**, 619–630 [CrossRef Medline](#)
69. Fontaine, D. A., and Davis, D. B. (2016) Attention to background strain is essential for metabolic research: C57BL/6 and the international knockout mouse consortium. *Diabetes* **65**, 25–33 [CrossRef Medline](#)
70. Zhao, S., Kusminski, C. M., Elmquist, J. K., and Scherer, P. E. (2020) Leptin: less is more. *Diabetes* **69**, 823–829 [CrossRef Medline](#)
71. Erion, K., and Corkey, B. E. (2018) β -Cell failure or β -cell abuse? *Front. Endocrinol. (Lausanne)* **9**, 532 [CrossRef Medline](#)
72. Smelt, M. J., Faas, M. M., de Haan, B. J., and de Vos, P. (2008) Pancreatic beta-cell purification by altering FAD and NAD(P)H metabolism. *Exp. Diabetes Res.* **2008**, 165360 [CrossRef Medline](#)
73. Van De Winkel, M., and Pipeleers, D. (1983) Autofluorescence-activated cell sorting of pancreatic islet cells: purification of insulin-containing B-cells according to glucose-induced changes in cellular redox state. *Biochem. Biophys. Res. Commun.* **114**, 835–842 [CrossRef Medline](#)

74. Redick, S. D., Leehy, L., Rittenhouse, A. R., Blodgett, D. M., Derr, A. G., Kucukural, A., Garber, M. G., Shultz, L. D., Greiner, D. L., Wang, J. P., Harlan, D. M., Bortell, R., and Jurczyk, A. (2020) Recovery of viable endocrine-specific cells and transcriptomes from human pancreatic islet-engrafted mice. *FASEB J.* **34**, 1901–1911 [CrossRef Medline](#)
75. Tennant, K. G., Lindsley, S. R., Kirigiti, M. A., True, C., and Kievit, P. (2019) Central and peripheral administration of fibroblast growth factor 1 improves pancreatic islet insulin secretion in diabetic mouse models. *Diabetes* **68**, 1462–1472 [CrossRef Medline](#)
76. Schindelin, J., Arganda-Carreras, I., Frise, E., Kaynig, V., Longair, M., Pietzsch, T., Preibisch, S., Rueden, C., Saalfeld, S., Schmid, B., Tinevez, J. Y., White, D. J., Hartenstein, V., Eliceiri, K., Tomancak, P., *et al.* (2012) Fiji: an open-source platform for biological-image analysis. *Nat. Methods* **9**, 676–682 [CrossRef Medline](#)